JPET Fast Forward. Published on May 27, 2010 as DOI: 10.1124/jpet.110.166009
This article has been copyedited and formatted. The final version may differ from this version.

Comparative Effects of the Endogenous Agonist GLP-1 7-36 Amide and a Small Molecule Ago-allosteric Agent 'Compound 2' at the GLP-1 Receptor

Karen Coopman, Yan Huang, Neil Johnston, Sophie J. Bradley, Graeme F. Wilkinson and Gary B. Willars

Department of Cell Physiology and Pharmacology, University of Leicester, Maurice Shock Medical Sciences Building, University Road, Leicester, LE1 9HN, UK (K.C., Y.H., N.J., S.J.B., G.B.W.); Biological Chemistry, Discovery Enabling Capabilities and Sciences, AstraZeneca, Alderley Park, Macclesfield, SK10 4TG, UK (G.F.W.)

Running title: GLP-1R small molecule allosteric agonist

Address for correspondence:

Dr. Gary B Willars

Department of Cell Physiology and Pharmacology, University of Leicester, Maurice Shock Medical Sciences Building, University Road, Leicester, LE1 9HN, U.K.

Tel.: +44 116 2297147

Fax: +44 116 2525045

Email: gbw2@le.ac.uk

Number of text pages: 44

Number of tables: 0

Number of figures: 11

Number of references: 36

Words in Abstract: 243

Words in Introduction: 435

Words in Discussion: 1500

Abbreviations:

BSA, bovine serum albumin; $[Ca^{2+}]i$, intracellular calcium concentration; Cpd2, compound 2 (6,7-dichloro-2-methylsulfonyl-3-*N*-*tert*-butylaminoquinoxaline); CTX, cholera toxin; DPP-IV, dipeptidyl peptidase-IV; EGFP, enhanced green fluorescent protein; FBS, foetal bovine serum; Fluo-4-AM, fluo-4-acetoxymethyl ester; FSK, forskolin; GLP-1, glucagon-like peptide; GLP-1R, GLP-1 receptor; GPCR, G-protein coupled receptor; hGLP-1R, human GLP-1R; IBMX, isobutylmethylxanthine; KHB, Krebs-HEPES buffer; NSB, non-specific binding; PTX, pertussis toxin; PKA, protein kinase A; VOCC, voltage-operated Ca^{2+} channels.

Recommended section assignment: Cellular and molecular

Abstract

Glucagon-like peptide-1 (GLP-1) mediates anti-diabetogenic effects through the GLP-1 receptor (GLP-1R), which is targeted for the treatment of type 2 diabetes. Small-molecule GLP-1R agonists have been sought due to difficulties with peptide therapeutics. Recently, 'compound 2' (6,7-dichloro-2-methylsulfonyl-3-*N*-*tert*-butylaminoquinoxaline) has been described as a GLP-1R allosteric modulator and agonist. Using HEK-293 cells expressing human GLP-1Rs we extended this work to consider the impact of compound 2 on G-protein activation, Ca^{2+} signaling and receptor internalisation and particularly to compare compound 2 and GLP-1 across a range of functional assays in intact cells. GLP-1 and compound 2 activated $G\alpha_s$ in cell membranes and increased cellular cAMP in intact cells, with compound 2 being a partial and almost full agonist respectively. GLP-1 increased intracellular [Ca^{2+}] by release from intracellular stores, which was mimicked by compound 2 with slower kinetics. In either intact cells or membranes, the orthosteric antagonist, exendin 9-39, inhibited GLP-1 cAMP generation but increased the efficacy of compound 2. GLP-1 internalised EGFP-tagged GLP-1Rs but the speed and magnitude evoked by compound 2 were less. Exendin 9-39 inhibited internalisation by GLP-1 and also surprisingly that by compound 2. Compound 2 displays GLP-1R agonism consistent with action at an allosteric site although an orthosteric antagonist increased its efficacy on cAMP and blocked compound 2-mediated receptor internalisation. Full assessment of the properties of compound 2 was potentially hampered by damaging effects that were particularly manifest in either longer-term assays with intact cells or acute assays with membranes.

JPET Fast Forward. Published on May 27, 2010 as DOI: 10.1124/jpet.110.166009
This article has not been copyedited and formatted. The final version may differ from this version.

Introduction

Glucagon like peptide-1 (GLP-1) is a potent modulator of insulin secretion that is released by L cells of the intestine in response to nutrient ingestion (Reimann et al., 2006). It is generated from proglucagon and exists as several truncated versions of the full-length peptide with the predominantly active form being GLP-1 7-36 amide (Orskov et al., 1994). GLP-1 exerts its actions through the GLP-1 receptor (GLP-1R), a Family B G-protein coupled receptor (GPCR). The GLP-1R is primarily coupled to $G\alpha_s$ and thereby mediates its effects through the generation of cAMP and its downstream targets, although coupling to $G\alpha_{i/o}$ and $G\alpha_{q/11}$ has been reported (Bavec et al., 2003; Hällbrink et al., 2001; Montrose-Rafizadeh et al., 1999). It is largely as a consequence of its ability to promote glucose-dependent insulin release from pancreatic β-cells (Holst et al., 1987; Holz et al., 1993) that it is an established target for the treatment of type 2 diabetes. Additionally, GLP-1 contributes to appropriate glucose homeostasis by increasing insulin biosynthesis, suppressing glucagon secretion, stimulating β-cell mass and suppressing appetite (Baggio and Drucker, 2007; Doyle and Egan, 2007; Holst, 2007). *In vivo*, GLP-1 has a plasma half-life of only 1-2 min as it is subject to rapid proteolytic degradation, particularly by the serine protease dipeptidyl peptidase-IV (DPP-IV), which cleaves the two N-terminal amino acid residues and renders the molecule biologically inactive (Kieffer et al., 1995; Mentlein et al., 1993).

The proteolytic degradation of GLP-1 presents considerable difficulties for therapeutic use and a range of DPP-IV-resistant analogues of GLP-1 such as Liraglutide (NN2211, Novo Nordisk), CJC-1131 (ConjuChem) and Exenatide (Exendin-4, AC2993, Amylin Pharmaceuticals/Eli Lilly & Co) (Meier and Nauck,

2005) have been developed. Although these agents have therapeutic potential, difficulties associated with the long-term administration of peptides have driven the search for small molecule, orally-active agonists of the GLP-1R. Recently, an exciting development has been the identification of a small molecule ligand of the GLP-1R, which not only increases the affinity of the GLP-1R for GLP-1 but is an agonist in its own right (Knudsen et al., 2007). This ago-allosteric agent, 'compound 2' (6,7-dichloro-2-methylsulfonyl-3-*N*-*tert*-butylaminoquinoxaline), stimulates cAMP production in membranes generated from BHK cells expressing the human GLP-1R (hGLP-1R), albeit with a bell-shaped concentration-response curve and also potentiates glucose-induced insulin release from pancreatic islets isolated from rodents. In the present study we have generated HEK-293 cell lines expressing either the hGLP-1R or this receptor with a C-terminal EGFP epitope-tag to further characterise signaling by compound 2, particularly to directly compare its actions with those of the major endogenous ligand, GLP-1 7-36 amide and to examine potential interactions between compound 2 and this orthosteric ligand.

JPET Fast Forward. Published on May 27, 2010 as DOI: 10.1124/jpet.110.166009
This article has not been copyedited and formatted. The final version may differ from this version.

Methods

Materials. All tissue culture plasticware was purchased from Nunc (VWR International, Lutterworth, U.K.). Media, foetal bovine serum (FBS), Lipofectamine 2000, oligonucleotides, Geneticin (G418), fluo-4-acetoxymethyl ester (fluo-4-AM), pluronic acid F-127 and hygromycin B were from Invitrogen (Paisley, U.K.). GLP-1 7-36 amide and exendin 9-39 were purchased from Bachem (Weil am Rhein, Germany) and compound 2 was synthesised at AstraZeneca UK (Alderley Edge, U.K.) based on the previously reported method (Knudsen et al., 2007). U73122 and U73343 (Bleasdale et al. 1990) were from Enzo Life Sciences (Exeter, U.K.). Protein A-Sepharose beads, [2,8-^{3}H]-adenosine 3', 5'-cyclic phosphate, ammonium salt (^{3}H-cAMP; 40 Ci/mmol) and [^{35}S]-GTPγS (1048 Ci/mmol) were obtained from Amersham Biosciences (GE Healthcare U.K. Ltd, Bucks., U.K.). Emulsifier Safe scintillation fluid, Whatman GF/B glass fibre filters and [^{125}I]-GLP-1 7-36 amide (2000Ci/mmol) were purchased from PerkinElmer LAS (U.K.) Ltd (Bucks., U.K.). Antibodies against the $G\alpha_{s}$- (sc-823) and $G\alpha_{i/o/t/z/gust}$- (sc-28586) protein subunits were purchased from Santa Cruz Biotechnology Inc. (CA, U.S.A.) and a monoclonal $G\alpha_{q/11}$ antibody was generated (Bundey and Nahorski, 2001) by Genosys Biotechnologies (Pampisford, U.K.) by inoculation of rabbits with the decapeptide (sequence QLNLKEYNLV) which is common to the C-terminus of both $G\alpha_{q}$ and $G\alpha_{11}$. The pEGFP-N1 plasmid encoding enhanced GFP (green fluorescent protein) for C-terminal tagging of the GLP-1R was from Clontech Laboratories (Saint-Germain-en-Laye, France). Restriction endonucleases were purchased from New England Biolabs (Hitchin, U.K.). DNA plasmid preparation and DNA gel extraction kits were from QIAGEN (Crawley, U.K.) and agarose powder was from BiozymT BV (Landgraaf,

The Netherlands). All other chemicals including pertussis toxin and cholera toxin (CTX) were purchased from Sigma-Aldrich (Gillingham, U.K.).

Cell culture and generation of cell lines with stable expression of hGLP-1Rs. HEK-Flp-In cells, wild-type HEK-293 cells, HEK-Flp-In cells with stable expression of the hGLP-1R (HEK-GLP-1R) or HEK-293 cells with stable expression of a C-terminal EGFP-tagged hGLP-1R (HEK-GLP-1R-EGFP) were routinely cultured in DMEM with high glucose (cat#41966) supplemented with 10% FBS in 80cm^2 or 175cm^2 tissue culture flasks at 37°C in a 5% CO_2 humidified atmosphere. The HEK-GLP-1R cell line was generated using the Flp-In system (Invitrogen, Paisley, U.K.) by transfection of HEK-Flp-In cells with pcDNA5/FRT containing the hGLP-1R (NCBI database: Accession NP_002053; Version, NP_002053.3; GI: 166795283) using Lipofectamine 2000 according to the manufacturer's instructions. Cells were then grown under selection using hygromycin B (400U/ml), clones selected by dilution cloning and screened for expression of the GLP-1R on the basis of [^{125}I]-GLP-1 7-36 amide binding and functional coupling to the generation of cAMP (see below). To generate the GLP-1R-EGFP cDNA construct, the coding sequence of the full length hGLP-1R containing Nhe1 and Xho1 restriction sites at the 5' and 3' ends respectively was cloned by PCR from the vector used for generation of the HEK-GLP-1R and ligated into the pEGFP-N1 vector. The construct contained an appropriately positioned Kozak sequence and start codon, and used the stop codon of the EGFP-containing vector. The recombinant plasmid was purified and the sequence confirmed by automated sequence analysis (PNACL, University of Leicester, Leicester, U.K.). Following transfection using Lipofectamine 2000, a stable cell line was generated by selection with G418 (1mg/ml). Clones were isolated using cloning

JPET Fast Forward. Published on May 27, 2010 as DOI: 10.1124/jpet.110.166009
This article has not been copyedited and formatted. The final version may differ from this version.

discs and following further growth the expression of GLP-1R-EGFP was assessed by immunoblotting of EGFP using standard methods, visualisation of EGFP fluorescence in live cells by confocal microscopy and cAMP responses to GLP-1. The stable cell line was maintained in media containing 200μg/ml G418.

Determination of ligand binding affinity and receptor expression levels. Membranes for binding experiments were prepared from confluent monolayers of cells in 80cm^2 flasks. The cells were washed with 5ml HBS (154mM NaCl, 10mM HEPES, pH 7.4, 37°C) and detached using harvesting buffer (154mM NaCl, 10mM HEPES, 5.4mM EDTA, pH 7.4, 37°C). Cells were collected by centrifugation (200g, 2 min, 4°C), and resuspended in 1ml of homogenization buffer (10mM HEPES, 10mM EDTA, pH 7.4). Cells were then sonicated (Sonifier Ultrasonic Cell Disruptor; Branson, CT, U.S.A.) at 30% of the maximal amplitude for 3×5s at ~30s intervals and centrifuged (30,000g, 4°C, 10 min). The pellets were resuspended in resuspension buffer (10mM HEPES, 0.1mM EDTA, pH 7.4), protein concentration adjusted to 2mg/ml and stored in aliquots at -80°C until assay. Binding assays were carried out in round-bottomed 5ml tubes in a total volume of 100μl in binding buffer (Hank's Balanced Salt Solution (HBSS) containing 20mM HEPES, 0.1% (w/v) bovine serum albumin (BSA), pH 7.4). Reactions contained membrane (12.5μg), [^{125}I]-GLP 7-36 amide (0.1nM) and GLP-1 7-36 amide at a range of concentrations (1μM-1pM). Binding was allowed to proceed to equilibrium by incubating at room temperature for 3 h. Membranes were then collected on Whatman GF/B glass fibre filters pre-soaked in 0.5% (v/v) polyethyleneimine using a Millipore vacuum manifold washed through with 2% (w/v) BSA. Ice-cold wash buffer (2ml; 25mM HEPES, 1.5mM $CaCl_2$, 1mM $MgSO_4$, 100mM NaCl, pH 7.4) was added the tube and

immediately poured onto the membrane under vacuum. The tube was then washed with a further 2ml wash buffer, which was added to the filter. Membranes were collected from tubes individually. Following harvesting, filters were allowed to dry and bound radioactivity determined by gamma-counter.

Determination of G protein activation. Determination of G-protein activation was carried out by [^{35}S]-GTPγS binding and immunoprecipitation of specific Gα-subunits as described elsewhere (Akam et al., 2001) using membranes prepared as described above. Briefly, membranes (75μg) were incubated with 1μM ($G\alpha_s$, $G\alpha_{q/11}$) or 10μM ($G\alpha_{i/o/t/z/gust}$) GDP and 1nM [^{35}S]-GTPγS in assay buffer (10mM HEPES, 100mM NaCl, 10mM $MgCl_2$, pH 7.4). Where appropriate, tubes contained 10μM GTPγS to determine non-specific binding or GLP-1 as stated. After incubation for 5 min at 30°C ($G\alpha_s$) or 37°C ($G\alpha_{q/11}$, $G\alpha_{i/o/t/z/gust}$), reactions were terminated with ice-cold assay buffer, and membranes pelleted by centrifugation. Pellets were solubilised, pre-cleared and incubated overnight at 4°C with 5μl of Gα-subunit specific anti-sera (1:100 dilutions). The resulting immune complexes were then isolated using protein A-Sepharose beads, collected by centrifugation and washed repeatedly. Beads were then resuspended in scintillation fluid and ^{35}S levels determined.

Determination of cAMP. ***Intact cells*** Cells were grown to confluent monolayers in 24-well plates coated with poly-D-lysine (0.1% w/v) and washed twice with 0.5ml Krebs-HEPES buffer (KHB, composition: 10mM HEPES; 4.2mM $NaHCO_3$; 11.7mM D-glucose; 1.18mM $MgSO_4 \cdot 7H_2O$; 1.18mM KH_2PO_4; 4.69mM KCl; 118mM NaCl; 1.3mM $CaCl_2 \cdot 2H_2O$; pH 7.4) containing 0.1% (w/v) BSA (KHB-BSA) before being incubated at 37°C for 10 min in KHB-BSA either with or without 500μM

isobutylmethylxanthine (IBMX) as indicated. Ligands (diluted in KHB-BSA) were added and the reactions terminated after the appropriate times by removal of the aqueous phase and addition of ice-cold 0.5M trichloroacetic acid to allow subsequent determination of intracellular cAMP levels. When levels of cAMP in the extracellular buffer were also measured, the KHB-BSA was removed and placed in a 1.5ml microfuge tube containing an equal volume of ice-cold 1M trichloroacetic acid.

Membranes The generation of cAMP was determined based on a previously published method (Dimitriadis et al., 1991). Following preparation of membranes exactly as described above, cAMP generation was determined in a total volume of 100µl containing: HEPES 10mM, $MgCl_2$ 12mM, NaCl 60mM, EDTA 1.2mM, BSA 1.2% w/v, ATP 480µM, IBMX 1.2mM, 20µg membrane. Preparations were untreated (basal), stimulated with either forskolin (10µM) or GTP (10µM) or stimulated with either GLP-1 7-36 amide (10nM or 100nM) or compound 2 (100µM) both in the presence of GTP (10µM). Where exendin 9-39 was present, this was at either 100nM or 1µM. Reactions were initiated by addition of membranes. After incubation with slow agitation (5 min, 30°C), reactions were terminated by addition of an equal volume of ice-cold 1M trichloroacetic acid.

In all cases, cAMP was extracted using a method identical to that for the extraction of Ins(1,4,5)P_3 (Willars and Nahorski, 1995) and levels determined by a competitive radioreceptor assay using binding protein purified from bovine adrenal glands (Brown et al., 1971) and related to cellular protein levels which were determined by Bradford assay.

Determination of changes in the intracellular Ca^{2+} concentration ($[Ca^{2+}]_i$). For determination of changes in $[Ca^{2+}]_i$ in cell populations, cells were grown to approximately 90% confluence in 96-well plates coated with poly-D-lysine (0.1% w/v) and loaded with 2μM fluo-4-AM diluted in KHB-BSA containing 0.036% (w/v) pluronic acid for 40 min at room temperature. Monolayers were then washed, equilibrated for 10 min and fluorescence recorded at 37°C in KHB-BSA as an index of $[Ca^{2+}]_i$ using a microplate reader (NOVOstar; BMG LABTECH, Aylesbury, U.K.) as previously described (Heding et al., 2002). For intracellular Ca^{2+} imaging, cells were plated into 6-well plates (approximately $0.5x10^6$ cells/well) containing 25mm diameter glass coverslips pre-coated with 0.1% (w/v) poly-D-lysine and allowed to adhere for 24-48 h. Cells were then loaded with fluo-4-AM as above and mounted in a perfusion chamber containing KHB heated to 37°C with a Peltier unit. The chamber volume was 0.5ml and where required was perfused at 5ml/min. Cells were imaged using an Ultra*VIEW* confocal microscope (PerkinElmer LAS, Beaconsfield, Bucks., U.K.) with a x40 oil-immersion objective lens and a 488nm Kr/Ar laser line. Emitted light was collected above 510nm and images captured at a rate of approximately 1 frame/sec using a CCD camera. Data analysis was carried out using the PerkinElmer Imaging Suite, with raw cytosolic fluorescence data exported to Microsoft Excel and expressed as F/F_o (fluorescence/basal fluorescence) for each cell.

Live-cell imaging of EGFP-tagged GLP-1Rs and determination of internalisation. HEK-GLP-1R-EGFP cells were grown on coverslips, rinsed with KHB and mounted in a perfusion chamber containing KHB at 37°C as described above. Cells were then imaged using an Ultra*VIEW* confocal microscope as described above. Ligand was added directly to the chamber in 200μl of pre-warmed KHB.

Vehicle controls were used as appropriate. Images were captured at 0, 2.5, 5, 10, 20, 30, 40, 50 and 60 min. For at least six individual cells on each coverslip and with at least three coverslips per experimental condition, fluorescence intensity was measured at a region of the plasma membrane and within the cytosolic compartment and a measure of internalisation derived using the equation: internalisation = $1-(Fm_t/Fc_t)/(Fm_b/Fc_b)$, where Fm_t and Fc_t represent the fluorescence intensity (in arbitrary units) at time t at the plasma membrane and in the cytosol respectively and Fm_b and Fc_b represent these parameters under basal conditions at the start of the experiment.

Assessment of cell viability by trypan blue exclusion. Cells were grown as monolayers in 24-well plates coated with poly-D-lysine (0.1% w/v) and washed twice with KHB-BSA before being incubated at 37°C for 10 min in KHB-BSA containing 500μM IBMX. Ligands in KHB-BSA were added for 90 min at 37°C before being aspirated and 500μl of 0.02% (w/v) trypan blue in KHB added. Cells were viewed using a Nikon ECLIPSE TE2000 inverted microscope with a x40 objective and bright field images captured using a Nikon Digital Sight camera and associated software (Nikon Instruments Europe, Badhoevedorp, The Netherlands). Cells excluding trypan blue after 5-10 min were regarded as viable whilst those in which the cytoplasm was blue were regarded as non-viable.

Data analysis. The K_d and B_{max} values were determined using standard analysis of homologous competition binding data using GraphPad Prism version 5.00 for Windows (GraphPad Software Inc., CA, U.S.A.). Concentration-response curves were also fitted using GraphPad Prism, according to a standard four parameter logistic

equation. Where the data were best described by a bell-shaped curve this was fitted using the appropriate equation in GraphPad Prism with nH1 and nH2 constrained to 1. The apparent pA_2 value of exendin 9-39 was calculated based on the equation: pA_2= log (DR-1) – log [antagonist] where DR is the dose ratio (Kenakin, 2004). All data are presented as mean+/±s.e.m., where n=3 unless otherwise stated.

Results

Signaling mediated by GLP-1 7-36 amide in HEK-GLP-1R cells. HEK-Flp-In cells with stable expression of the hGLP-1R (HEK-GLP-1R cells) were initially characterised by examining the binding and signaling of GLP-1 7-36 amide. Homologous competition binding revealed a K_D for GLP-1 7-36 amide of -8.95±0.09 $\log_{10}$ M and a B_{max} value of 1061±223 fmol/mg protein. G-protein activation by GLP-1 7-36 amide in membranes prepared from HEK-GLP-1R cells was assessed by specific Gα immunoprecipitation and determination of bound [^{35}S]-GTPγS following agonist challenge. Under these circumstances, using a concentration of GLP-1 7-36 amide that was maximal for both cAMP and intracellular Ca^{2+} responses (30nM; see below), an increased association of ^{35}S was observed with $G\alpha_s$ but not with either $G\alpha_{i/o}$ or $G\alpha_{q/11}$ (Fig. 1a). The ability of the $G\alpha_{i/o}$ and $G\alpha_{q/11}$ antibodies to immunoprecipitate the relevant activated G-proteins was confirmed using membranes prepared from CHO cell lines recombinantly expressing either $G\alpha_{i/o}$-coupled muscarinic M_2 receptors or $G\alpha_{q/11}$-coupled muscarinic M_3 receptors (Burford et al., 1995) challenged with the muscarinic receptor agonist methacholine (1mM; data not shown).

GLP-1 7-36 amide stimulated a time-dependent, robust increase in cAMP production in intact HEK-GLP-1R cells, which in the absence of the phosphodiesterase inhibitor (IBMX) reached a maximal after approximately 15 min (Fig. 1b). The increase in cAMP was also concentration-dependent with a pEC_{50} at 10 min of 10.07±0.14 (85pM) (Fig. 1c). Pre-treatment of cells for 10 min with the GLP-1R antagonist, exendin 9-39 (100nM), and its continued presence during stimulation with GLP-1 7-

36 amide resulted in a dextral shift of the concentration-response curve (Fig. 1c) with an apparent pA_2 value for exendin 9-39 of 7.29±0.07 (52nM). Pre-treatment of cells with exendin 9-39 for 60 min did not significantly alter the apparent pA_2 value (7.33±0.16, 47nM, graphs not shown). Although CTX activates $G\alpha_s$, extended treatment can down-regulate $G\alpha_s$ and can therefore, in some circumstances, be used to assess involvement in cellular responses (Seidel et al., 1999). Here, 24 h treatment of HEK-GLP-1R cells with CTX reduced cAMP generation in response to a maximal concentration of GLP-1 7-36 amide (Fig. 1d). However, CTX treatment markedly elevated 'basal' levels of cAMP in the absence of ligand and had no effect on cAMP generation by a lower concentration (0.1nM) of GLP-1 7-36 amide (Fig. 1d).

In fluo-4-loaded populations of HEK-GLP-1R cells, GLP-1 7-36 amide evoked a rapid increase in fluorescence (reflecting an increase in $[Ca^{2+}]_i$), which was followed by a slower decline (Fig. 2a). The maximal response following addition of GLP-1 7-36 amide was concentration-dependent (Fig. 2a and b) with a pEC_{50} of 10.18±0.16 (67pM). In the presence of 100nM exendin 9-39, the pEC_{50} was relatively unaffected (control 10.18±0.16 vs. 9.79±0.11 in the presence of exendin 9-39) but the curve was partially collapsed (E_{max} reduced to 79±3% of control) (Fig. 2b). The Ca^{2+} response to GLP-1 7-36 amide was unaffected by removal of extracellular Ca^{2+} but was almost abolished by pre-treatment with the sarco/endoplasmic reticular Ca^{2+}-ATPase inhibitor thapsigargin to deplete intracellular Ca^{2+} stores (Fig. 2c). Pre-treatment of cells with either the putative inhibitor of phospholipase C, U73122, or its aminosteroid negative control, U73343, or overnight treatment with pertussis toxin to ADP-ribosylate and inactivate $G\alpha_{i/o}$ proteins had no effect on the Ca^{2+} responses to GLP-1 7-36 amide (Fig. 2d). Experiments with U73122 and U73343 were performed

JPET Fast Forward. Published on May 27, 2010 as DOI: 10.1124/jpet.110.166009
This article has not been copyedited and formatted. The final version may differ from this version.

in nominally Ca^{2+}-free buffer to avoid potential effects of these compounds on Ca^{2+} entry across the plasma membrane (Werry et al., 2003). Single-cell, confocal imaging of fluo-4-loaded HEK-GLP-1R cells demonstrated that GLP-1 7-36 amide increased fluorescence in all cells and particularly at sub-maximal concentrations was sometimes associated with oscillatory changes in $[Ca^{2+}]_i$ (Fig. 2e and data not shown).

Signaling mediated by compound 2 in HEK-GLP-1R cells. Challenge of membranes prepared from HEK-GLP-1R cells with compound 2 in the presence of [^{35}S]-GTPγS resulted in a concentration-dependent increase in the association of ^{35}S with $G\alpha_s$ (Fig. 3a). However, the concentration-response curve was bell-shaped, with the response reaching a maximum at 10μM and declining thereafter. The pEC_{50} of the rising phase of this curve was 5.36±0.16 (4.4μM, n=4) with a maximal response of 16±2% of the response to 30nM GLP-1 7-36 amide. Compound 2 had no effect on the association of ^{35}S with either $G\alpha_{q/11}$ or $G\alpha_{i/o}$ (Fig. 3b and c). Neither compound 2 nor GLP-1 7-36 amide stimulated an increase in the association of ^{35}S with $G\alpha_s$ in membranes prepared from HEK-Flp-In cells (Fig. 3d) or wild-type HEK-293 cells (data not shown).

Challenge of HEK-GLP-1R cells for 10 min with compound 2 resulted in a concentration-dependent increase in intracellular cAMP levels (Fig. 4a) with a pEC_{50} of 6.23±0.07 (0.59μM). The maximum cAMP production in response to compound 2 was 88±8% of that produced by a maximal concentration of GLP-1 (30nM). Neither compound 2 nor GLP-1 7-36 amide stimulated an increase in cAMP in HEK-Flp-In cells (Fig. 4b) or wild-type HEK-293 cells (data not shown). The response to a submaximal (1μM) concentration of compound 2 was time-dependent, showing an

JPET Fast Forward. Published on May 27, 2010 as DOI: 10.1124/jpet.110.166009
This article has not been copyedited and formatted. The final version may differ from this version.

increase in levels up to approximately 15 min but a subsequent rapid decline in the absence of IBMX (Fig. 4c). In contrast to the original study on compound 2 that reported a bell-shaped concentration-response curve (Knudsen et al., 2007), that shown here was clearly sigmoidal. However, our assay was much shorter and when the assay was extended to 90 min in line with the original study, the concentration-dependence of compound 2-mediated cAMP responses showed a very pronounced bell-shaped relationship, which reached a maximum at approximately 3μM and a dramatic decline at higher concentrations (Fig. 4d). The potency of compound 2 for this response was approximated by fitting a truncated curve with concentrations between 0.001μM and 3μM. This gave a pEC_{50} value of 6.18±0.05 (0.66μM, n=4) which was not significantly different from the value determined at 10 min. Stimulating cells for 90 min with GLP-1 7-36 amide did not result in a bell-shaped concentration-response curve. The curve was sigmoidal with a pEC_{50} 9.94±0.09 (graph not shown), which was not significantly different from that at 10 min (10.07±0.14).

In the experiments measuring cAMP described above, the extracellular buffer was removed prior to terminating the reaction to allow the measurement of intracellular cAMP levels. To assess whether the downward slope of the bell-shaped concentration-response curve to compound 2 at 90 min of stimulation was a consequence of reduced cAMP generation or reduced cellular retention we measured both intracellular and extracellular levels of cAMP. Exposure of HEK-GLP-1R cells to either forskolin, approximately EC_{50} (100pM) or high (30nM) concentrations of GLP-1 7-36 amide or an approximate EC_{50} concentration of compound 2 (1μM) resulted in similar proportions of extracellular and intracellular cAMP (Fig. 5a). In

contrast, cAMP measured in response to challenge with a high (100μM) concentration of compound 2 was predominantly extracellular and, as expected from the bell-shaped concentration-response curve, considerably lower than levels generated by the lower concentration of compound 2 (Fig. 5a). After 90 min of challenge with high concentrations of compound 2, cells lost their flattened morphology and rounded-up. Thus, cellular morphology was assessed along with a determination of viability using trypan blue exclusion. Treatment of cells with vehicle (5% v/v DMSO) or a low concentration of compound 2 (10nM) did not affect cell morphology or viability (Fig 5b). At an approximately EC_{50} concentration of compound 2 (1μM), the cells had a much more rounded morphology but remained viable as judged by their ability to exclude trypan blue. At higher concentrations of compound 2 (eg. 100μM; Fig. 5b), in addition to rounding up, cells were no longer able to exclude trypan blue indicating a loss of viability. These higher concentrations of compound 2 had similar effects on HEK-Flp-In cells (Fig. 5b) and wild-type HEK-293 cells not expressing the GLP-1R (data not shown). Concentrations of compound 2 greater than 10μM also inhibited forskolin-stimulated cAMP accumulation (Fig. 5c). Overnight treatment of HEK-GLP-1R cells with pertussis toxin did not influence forskolin-stimulated cAMP generation and did not influence the inhibitory effect of a high concentration of compound 2 (100μM) on this forskolin-stimulated cAMP generation (Fig. 5d).

The cAMP response to a maximal concentration of compound 2 (10μM) was only partially attenuated by CTX treatment (Fig. 6a). In addition, the cAMP response to an approximately EC_{50} concentration of compound 2 (1μM) was unaffected by CTX treatment (Fig. 6a). These effects of CTX that were dependent on agonist concentration were clearly shown when full concentration-response curves for

JPET Fast Forward. Published on May 27, 2010 as DOI: 10.1124/jpet.110.166009
This article has not been copyedited and formatted. The final version may differ from this version.

compound 2-mediated cAMP generation in the absence and presence of pre-treatment with CTX were constructed (Fig. 6b). These experiments again showed that CTX caused a substantial increase in 'basal' levels of cAMP (Fig. 6a and b).

In contrast to the dextral shift of the cAMP concentration-response curve for GLP-1 7-36 amide by pre-treatment with 100nM exendin 9-39 (Fig. 1c), this orthosteric antagonist did not cause a similar shift in the concentration-response curve for compound 2-mediated cAMP generation. The presence of exendin 9-39 did, however, increase the E_{max} of compound 2 to 137±17% of control (n=4) without a significant effect on the pEC_{50} value (control 6.02±0.07 vs. 6.17±0.09 with exendin 9-39, n=4) (Fig. 7a). At progressively higher concentrations of exendin 9-39 (up to 3μM), the antagonist caused significant reductions in the cAMP response to an approximate EC_{50} concentration of GLP- 7-36 amide (100pM). However, these increasing concentrations of exendin 9-39 only enhanced the magnitude of the response to an approximately EC_{50} concentration of compound 2 (1μM) (Fig. 7b). In order to investigate potential interactions between compound 2 and GLP-1 7-36 in our cell line, similar experiments were performed to those described in the original identification of compound 2 (Knudsen et al., 2007). Thus, HEK-GLP-1R cells were co-stimulated for 10 min and changes in intracellular cAMP levels assessed. As also shown above, compound 2 acted as an agonist and caused a concentration-dependent increase in cAMP levels in the absence of GLP-1 7-36 amide (Fig. 7c; control). The E_{max} of the response to GLP-1 7-36 amide was identical in the presence and absence of compound 2. Co-stimulation of the cells with 10nM GLP-1 7-36 amide and 100μM forskolin resulted in a response which was 22±3% greater than GLP-1 7-36 amide alone (data not shown), indicating that the lack of additivity at E_{max} values was

JPET Fast Forward. Published on May 27, 2010 as DOI: 10.1124/jpet.110.166009
This article has not been copyedited and formatted. The final version may differ from this version.

not through an inability to detect further increases. Although the E_{max} was unaffected, the potency of GLP-1 7-36 amide was significantly reduced with increasing concentrations of compound 2 ($p<0.05$, F-test).

Addition of compound 2 to populations of fluo-4-loaded cells caused an initial rapid increase in the fluorescence signal that was a consequence of the fluorescent properties of the compound (Fig. 8a) as this increase was apparent on the addition to buffer in the absence of cells and fluo-4 (data not shown). Compound 2 evoked a concentration-dependent, slowly rising increase in $[Ca^{2+}]_i$ that was longer lasting than that in response to GLP-1 7-36 amide (Fig. 8a and 8b). The time to the maximal change in fluorescence was greater following addition of compound 2 (100μM, 36.4±10.0s, n=4) than following GLP-1 7-36 amide (100nM, 21.6±1.5s, n=4). We were unable to determine the potency of compound 2 for this response as solubility and toxicity issues with DMSO limited the use of higher concentrations. The initial rapid increase in fluorescence on addition of compound 2 (100μM) was present in HEK-Flp-In cells (Fig. 8c). Compound 2 also caused a small gradual increase in fluorescence in these HEK-Flp-In cells (Fig. 8c) and wild-type HEK-293 cells (data not shown) but this was distinguishable from responses in cells expressing the GLP-1R (Fig. 8a). The maximal Ca^{2+} response to 100μM compound 2 was abolished by pretreatment of cells with thapsigargin (2μM, 5 min) (Fig. 8d) but unaffected by removal of extracellular Ca^{2+} (Fig. 8d). Pre-treatment of cells with either U73122 or U73343 (and subsequent challenge with compound 2 in the absence of extracellular Ca^{2+}) or alternatively overnight treatment with pertussis toxin had no effect on the Ca^{2+} responses to compound 2 (Fig. 8e). Exendin 9-39 (100nM, 10 min pre-treatment) had no significant effect on the maximal $[Ca^{2+}]_i$ change in response to

100μM compound 2 (60.8±5.6% and 71.3±2.7% of the response to 100nM GLP-1 7-36 amide in the absence and presence of exendin 9-39 respectively).

Receptor internalisation. Stable expression of a C-terminal EGFP-tagged hGLP-1R (GLP-1R-EGFP) in HEK-293 cells resulted in a cell line (HEK-GLP-1R-EGFP) with a K_D for GLP-1 7-36 amide of -8.98±0.14 $\log_{10}$ M and a B_{max} value of 951±213 fmol/mg protein. In parallel experiments using the HEK-GLP-1R and HEK-GLP-1R-EGFP cell lines, the potencies of GLP-1 7-36 amide (pEC_{50} values 10.40±0.27 and 10.41±0.18 respectively) and compound 2 (pEC_{50} values 6.00±0.13 and 6.02±0.03 respectively) were not different between the cell lines, although the E_{max} values were lower in the HEK-GLP-1R-EGFP cell line (E_{max} values for GLP-1 7-36 amide and compound 2 were 53% and 27% of those in the HEK-GLP-1R cell line) (Fig. 9).

Confocal imaging of HEK-GLP-1R-EGFP cells revealed intense, continuous plasma membrane fluorescence (Fig. 10a, 0 min). Challenge of cells with GLP-1 7-36 amide (100nM) resulted in marked internalisation of fluorescence. In the first 10 min fluorescence aggregated in small discrete patches at the plasma membrane and this was followed by movement of these puncta into the interior of the cell where they coalesced in discrete regions (Fig. 10a). Quantification of changes in plasma membrane and cytosolic fluorescence indicated that internalisation was maximal by approximately 30 min (Fig. 10b) and that relatively little fluorescence remained at the cell membrane (Fig. 10a and b). Over the 60 min period, a very minor amount of internalisation occurred in the presence of DMSO (0.1% v/v) (Fig. 10a and b) but this was not different from cells in buffer alone (data not shown). The GLP-1 receptor antagonist, exendin 9-39 (100nM), had no impact on the distribution of fluorescence

over and above that seen in vehicle-treated cells (Fig. 10a and b). However, preincubation of cells with exendin 9-39 (100nM) for 10 min reduced the rate and extent of internalisation mediated by GLP-1 7-36 amide (100nM) (Fig. 10a and b). Following addition of compound 2 (10μM) there was a delay of approximately 10 min before the initiation of detectable internalisation, which then progressed at a slower rate and was less extensive (67%) than that mediated by GLP-1 7-36 amide (Fig. 10a and b). Preincubation of cells with exendin 9-39 (100nM) for 10 min reduced the rate and extent of internalisation mediated by compound 2 (10μM) to essentially basal levels (Fig. 10a and b). Co-application of GLP-1 7-36 amide (100nM) and compound 2 (10μM) resulted in an initial internalisation that was similar to that seen in cells treated with GLP-1 7-36 amide alone (Fig. 10b). However, between 20 and 60 min the extent of internalisation was less than that with GLP-1 7-36 amide alone but still greater than that with compound 2 alone.

Given the ability of exendin 9-39 to inhibit compound 2-mediated internalisation of the GLP-1R-EGFP we examined whether this capacity to maintain cell-surface receptor was responsible for the ability of exendin 9-39 to enhance compound 2-mediated cAMP generation by the GLP-1R. Initially we demonstrated that exendin 9-39 did indeed enhance compound 2-mediated cAMP generation in HEK-GLP-1R-EGFP cells. Thus, exendin 9-39 had little effect on the potency of compound 2 but increased the E_{max} from 84±5% to 100±6% of the GLP-1 7-36 amide response in these cells (Fig. 11a), mimicking the effect observed in HEK-GLP-1R cells. In a membrane assay of cAMP generation, in which regulation of receptor internalisation would not contribute to differences in cAMP generation, exendin 9-39 inhibited

cAMP generation in response to a sub-maximal concentration of GLP-1 and caused a modest but significant increase in the compound 2-mediated response (Fig. 11b).

Discussion

The GLP-1R is a target for the treatment of type 2 diabetes and whilst peptides can offer high potency agonism they do not provide ideal therapeutics. The exciting recent identification of small molecule allosteric (Knudsen et al., 2007) and orthosteric agonists (Chen et al., 2007) provides hope for the development of high affinity, orally active compounds having the full spectrum of activity at the GLP-1R and clinical applicability. Here we have examined agonism of 6,7-dichloro-2-methylsulfonyl-3-*N*-*tert*-butylaminoquinoxaline (compound 2; Knudsen et al., 2007) for functionally important signaling events and compared these with the primary endogenous orthosteric ligand of the GLP-1R, GLP-1 7-36 amide.

GPCRs belonging to Family B, for which endogenous ligands are known, couple to $G\alpha_s$, adenylyl cyclase and cAMP generation. The GLP-1R is no exception and evidence supports such coupling by endogenous or recombinantly expressed receptors in different cells. Although coupling to $G\alpha_{q/11}$ and $G\alpha_i$, has been reported; particularly by recombinant GLP-1Rs (Bavec et al., 2003; Hällbrink et al., 2001; Montrose-Rafizadeh et al., 1999), we show using immunoprecipitation of G-proteins that GLP-1 7-36 amide activates $G\alpha_s$ but not $G\alpha_{q/11}$ or $G\alpha_i$ in our cell line. Further, GLP-1 7-36 amide robustly increases intracellular cAMP. Compound 2, shown previously to generate cAMP in membrane-based assays with biphasic concentration-dependence (Knudsen et al., 2007) also activated $G\alpha_s$ in membranes and generated cAMP in intact cells. The concentration-dependence of $G\alpha_s$ activation and cAMP generation in long (90 min) but not short (10 min) assays was biphasic. Curves of this shape are likely due to adverse effects of compound 2, as in both membranes (Knudsen et al., 2007) and cells (Fig 5c), higher concentrations inhibit forskolin-

mediated cAMP generation. Although estimates may be compromised by adverse effects, data indicate that compound 2 activates $G\alpha_s$ with low potency (4.4μM) and low efficacy (16% of GLP-1 7-36 amide) and elevates cAMP with low potency (0.59μM) but higher efficacy (88% of GLP-1 7-36 amide). These differences in potency and efficacy may reflect signal amplification. Adverse effects of compound 2 are independent of GLP-1R expression and include effects independent of cell viability, one manifestation of which is a direct effect on receptors. For example, in a 1 h assay at 37°C, 10μM compound 2 reduced binding of the muscarinic receptor antagonist 1-[*N-methyl*-^{3}H]scopolamine methyl chloride to muscarinic M_3 receptors stably expressed in HEK-293 cells (27±3% of control, n=3) (*see* Tovey and Willars, 2004 for description of cell line). These adverse effects are a likely consequence of the chemical nature of compound 2 (Knudsen et al., 2007).

Here we show that like the endogenous ligand, compound 2 elevates $[Ca^{2+}]_i$ by release from thapsigargin-sensitive intracellular stores, albeit with slower kinetics. Although compound 2 potency and efficacy could not be determined, GLP-1 7-36 amide elevated $[Ca^{2+}]_i$ and cAMP with similar potency, consistent with other recombinant systems (Wheeler et al., 1993; Widmann et al., 1994; Syme et al., 2006). Ca^{2+} signaling by the GLP-1R reflects an important physiological role and is likely to be a critical property of therapeutics targeting this receptor. Ca^{2+} is key for insulin release from pancreatic β-cells where there is a complex interplay between pathways evoking Ca^{2+} responses (Doyle and Egan, 2007; Holst, 2007). GLP-1-mediated Ca^{2+} signaling in β-cells includes protein kinase A (PKA)-dependent inhibition of K_{ATP} channels, which at higher glucose concentrations causes membrane depolarisation and activation of voltage-operated Ca^{2+} channels (VOCCs). Additionally, PKA may

directly regulate VOCCs and K_v channels, enhancing Ca^{2+} entry. Adenylyl cyclase activation also facilitates insulin exocytosis through a PKA-dependent mobilisation of intracellular Ca^{2+} stores, an Epac-dependent sensitization of ryanodine receptors and/or a PKA-dependent sensitization of IP_3 receptors (Doyle and Egan, 2007). Furthermore, at low physiological concentrations of GLP-1, insulin-secretion is PKA-independent but Ca^{2+}-dependent (Shigeto et al., 2008). Compound 2 clearly provokes glucose-dependent insulin release (Knudsen et al., 2007) although the contributions of different Ca^{2+} signaling mechanisms are unknown.

Our data suggest that GLP-1R-mediated responses are not downstream of either $G\alpha_{q/11}$ or $G\alpha_{i/o}$ activation. Although coupling to all G-proteins has not been examined, data are at least in-line with signaling through $G\alpha_s$ activation. This is consistent with coupling of the endogenous receptor in β-cell lines (Widmann et al., 1994) and the recombinant receptor in some (Widmann et al., 1994) but not all (Wheeler et al., 1993) cell types. Assessment of the involvement of $G\alpha_s$ using CTX treatment was hampered by the ongoing stimulatory effects of the toxin even following 20-24 h of treatment. Substantial residual agonist-mediated cAMP generation also highlighted the difficulty of using this toxin to assess the role of $G\alpha_s$ in other signalling events. The precise mechanisms by which GLP-1R activation releases Ca^{2+} from stores following activation by either agonist is unclear. Pretreatment with pertussis toxin had no effect on Ca^{2+} signalling. Furthermore, neither agonist caused accumulation of ^{3}H-inositol phosphates over 30 min against a lithium-block of inositol monophosphatase activity (data not shown) (*see* Willars and Nahorski, 1995) indicating an absence of phospholipase C activity. Despite difficulties associated with the use of U73122 (Werry et al., 2003), the lack of effect

of this putative phospholipase C inhibitor on Ca^{2+} signaling further supports a lack of its involvement in Ca^{2+} responses.

GLP-1 7-36 amide-mediated cAMP generation was inhibited by the orthosteric competitive antagonist, exendin 9-39 (Göke et al., 1993; Thorens et al., 1993) with an apparent pA_2 of 7.29 (52nM). Although greater than the reported K_d (~1nM) (Thorens et al., 1993), our estimate is from very different conditions in a functional assay without full Schild analysis. Exendin 9-39 did not inhibit compound 2-mediated cAMP generation, consistent with agonism at an allosteric site (Knudsen et al., 2007), which has been speculated to be a cavity near TM5 and TM6 (Lin and Wang, 2009). Compound 2 increases GLP-1 affinity (Knudsen et al., 2007) and it was surprising that compound 2 reduced GLP-1 potency for cAMP generation. Although these data could indicate that compound 2 is a partial agonist at the orthosteric site or an allosteric agonist with negative cooperativity, we believe such interpretation is severely compromised by adverse effects of compound 2, which manifest here as reduced GLP-1 potency. Our data are also inconsistent with the previous report that compound 2 does not influence GLP-1 potency (Knudsen et al., 2007). However, in that study, the potencies of GLP-1 and compound 2 were much higher, consistent with greater levels of receptor expression and therefore much lower levels of compound 2 were used, which may have had rather more limited adverse effects.

Surprisingly, exendin 9-39 increased the E_{max} of compound 2-mediated cAMP generation in both intact cell and membrane-based assays. Whilst compound 2 can increase orthosteric agonist affinity (Knudsen et al., 2007), it is unclear how increased

efficacy occurs. Exendin 9-39 may facilitate the stabilisation of a more active receptor conformation by compound 2 or protect against the adverse effects of compound 2.

Compared to compound 2, receptor internalisation mediated by GLP-1 7-36 amide was both faster and greater. The mechanisms underlying GLP-1R internalisation are unclear. In HEK-293 and MIN6 cells internalisation is an arrestin-independent, caveolin-mediated process (Syme et al., 2006). However, GRK-dependent receptor phosphorylation and β-arrestin 2-dependent internalisation, presumably via a clathrin-dependent pathway, has been implicated in other cells (Widmann et al., 1995; Vázquez et al., 2005; Jorgensen et al., 2005). Internalisation of GLP-1-bound receptors may be important for ligand dissociation and receptor re-sensitisation. Further, for some receptors, internalisation is critical for coupling to specific pathways, particularly G-protein-independent signaling, which can include the mitogen-activated protein kinases. We have not explored the mechanisms or consequences of internalisation here and it is unclear if they are identical following activation by allosteric and orthosteric agonists. The observed differences in internalisation could reflect partial agonism of compound 2 or differences in receptor occupancy. Thus, although we selected agonist concentrations that were maximal and approximately equally effective on cAMP generation (10 min assay), receptor occupancies may differ. Compound 2 toxicity prevented use of supra-maximal concentrations to overcome this problem. Toxicity could also limit internalisation, even at lower concentrations, although this is not supported by the ability of GLP-1 7-36 amide to enhance internalisation in the presence of compound 2. Surprisingly, exendin 9-39 inhibited compound 2-mediated receptor internalisation. It is possible

that exendin 9-39 generates a receptor conformation unable to internalise, even in the presence of an allosteric agonist but this is not associated with reduced signaling. Indeed exendin 9-39 enhanced compound 2 efficacy but this was unrelated to reduced internalisation as it was present in membrane cAMP assays. It is unclear if exendin 9-39 reduces processes associated with desensitisation such as receptor phosphorylation, which would promote signaling and reduce arrestin-dependent internalisation.

Thus, compound 2 displays agonism at the GLP-1R that is qualitatively similar to that of the major endogenous ligand, GLP-1 7-36 amide, but quantitatively different. Although evidence suggests an allosteric mechanism for compound 2, enhanced efficacy and reduced receptor internalisation in the presence of the orthosteric antagonist suggest complex interactions between the allosteric and orthosteric sites. The challenge is to design potent small molecule GLP-1R agonists in which toxicity does not compromise the therapeutic window and allows full assessment of their pharmacology independent of toxicity.

Acknowledgements

Our thanks go to Ruth Wallis (AstraZeneca, Alderely Park Macclesfield, U.K.) for generating the HEK-GLP-1R cell line and Dr. Chris Langmead (Heptares Therapeutics Ltd., Welwyn Garden City, U.K.) for expert help in the analysis of compound 2 interactions with GLP-1 7-36 amide.

References

Akam EC, Challiss RA, and Nahorski SR (2001) $G_{q/11}$ and $G_{i/o}$ activation profiles in CHO cells expressing human muscarinic acetylcholine receptors: dependence on agonist as well as receptor-subtype. *Br J Pharmacol* **132:** 950-958.

Baggio LL, and Drucker DJ (2007) Biology of incretins: GLP-1 and GIP. *Gastroenterology* **132:** 2131-2157.

Bavec A, Hällbrink M, Langel U, and Zorko M (2003) Different role of intracellular loops of glucagon-like peptide-1 receptor in G-protein coupling. *Regul Peptides* **111:** 137-144.

Bleasdale JE, Thakur NR, Gremban RS, Bundy GL, Fitzpatrick FA, Smith RJ, and Bunting S (1990) Selective inhibition of receptor-coupled phospholipase C-dependent processes in human platelets and polymorphonuclear neutrophils. *J Pharmacol Exp Ther* **255:** 756-768.

Brown BL, Albano JD, Ekins RP, and Sgherzi AM (1971) A simple and sensitive saturation assay method for the measurement of adenosine 3':5'-cyclic monophosphate. *Biochem J* **121:** 561-562.

Bundey RA, and Nahorski SR (2001) Homologous and heterologous uncoupling of muscarinic M_3 and α_{1B} adrenoceptors to $G\alpha_{q/11}$ in SH-SY5Y human neuroblastoma cells. *Br J Pharmacol* **134:** 257–264.

Burford NT, Tobin AB, and Nahorski SR (1995) Differential coupling of m1, m2 and m3 muscarinic receptor subtypes to inositol 1,4,5-trisphosphate and adenosine

3',5'-cyclic monophosphate accumulation in Chinese hamster ovary cells. *J Pharmacol Exp Ther* **274:** 134-142.

Chen D, Liao J, Li N, Zhou C, Liu Q, Wang G, Zhang R, Zhang S, Lin L, Chen K, Xie X, Nan F, Young AA, and Wang M-W (2007) A nonpeptidic agonist of glucagon-like peptide 1 receptors with efficacy in diabetic db/db mice. *Proc Nat Acad Sci U.S.A.* **104:** 943-948.

Dimitriadis GD, Richards SJ, Parry-Billings M, Leighton B, Newsholme EA, and Challiss RAJ (1991) β-adrenoceptor-agonist and insulin actions on glucose metabolism in rat skeletal muscle in different thyroid states. *Biochem J* **278:** 587-593.

Doyle ME, and Egan JM (2007) Mechanisms of action of glucagon-like peptide 1 in the pancreas. *Pharmacol Ther* **113:** 546-593.

Göke R, Fehmann H-C, Linn T, Schmidt H, Krause M, Eng J, and Göke B (1993) Exendin-4 is a high potency agonist and truncated exendin-(9-39)-amide an antagonist at the glucagon-like peptide 1-(7-36)-amide receptor of insulin-secreting β-cells. *J Biol Chem* **268:** 19650-19655.

Hällbrink M, Holmqvist T, Olsson M, Östenson CG, Efendic S, and Langel U (2001) Different domains in the third intracellular loop of the GLP-1 receptor are responsible for $G\alpha_s$ and $G\alpha_i/G\alpha_o$ activation. *Biochim Biophys Acta Protein Struct Mol Enzymol* **1546:** 79-86.

Heding A, Elling CE, and Schwartz TW (2002) Novel method for the study of receptor Ca^{2+} signalling exemplified by the NK1 receptor. *J Recept Signal Transduction* **22:** 241 - 252.

Holst JJ (2007) The physiology of glucagon-like peptide 1. *Physiol Rev* **87:** 1409-1439.

Holst JJ, Orskov C, Nielsen OV, and Schwartz TW (1987) Truncated glucagon-like peptide I, an insulin-releasing hormone from the distal gut. *FEBS Lett* **211:** 169-174.

Holz GGt, Kuhtreiber WM, and Habener JF (1993) Pancreatic beta-cells are rendered glucose-competent by the insulinotropic hormone glucagon-like peptide-1(7-37). *Nature* **361:** 362-365.

Jorgensen R, Martini L, Schwartz TW, and Elling CE (2005) Characterization of glucagon-like peptide-1 receptor β-arrestin 2 interaction: a high affinity receptor phenotype. *Mol Endocrinol* **19:** 812-823.

Kenakin T (2004) *A Pharmacology Primer: Theory, Application, and Methods*. Elsevier Academic Press.

Kieffer TJ, McIntosh CH, and Pederson RA (1995) Degradation of glucose-dependent insulinotropic polypeptide and truncated glucagon-like peptide 1 in vitro and in vivo by dipeptidyl peptidase IV. *Endocrinology* **136:** 3585-3596.

Knudsen LB, Kiel D, Teng M, Behrens C, Bhumralkar D, Kodra JT, Holst JJ, Jeppesen CB, Johnson MD, de Jong JC, Jorgensen AS, Kercher T, Kostrowicki J, Madsen P, Olesen PH, Petersen JS, Poulsen F, Sidelmann UG, Sturis J, Truesdale L, May J, and Lau J (2007) Small-molecule agonists for the glucagon-like peptide 1 receptor. *Proc Nat Acad Sci U.S.A.* **104:** 937-942.

Lin F, and Wang R (2009) Molecular modeling of the three-dimensional structure of GLP-1R and its interactions with several agonists. *J Mol Model* **15:** 53-65.

Meier JJ, and Nauck MA (2005) Glucagon-like peptide 1 (GLP-1) in biology and pathology. *Diabetes-Metab Rev* **21:** 91-117.

Mentlein R, Gallwitz B, and Schmidt WE (1993) Dipeptidyl-peptidase IV hydrolyses gastric inhibitory polypeptide, glucagon-like peptide-1(7-36)amide, peptide histidine methionine and is responsible for their degradation in human serum. *Eur J Biochem* **214:** 829-835.

Montrose-Rafizadeh C, Avdonin P, Garant MJ, Rodgers BD, Kole S, Yang H, Levine MA, Schwindinger W, and Bernier M (1999) Pancreatic glucagon-like peptide-1 receptor couples to multiple G proteins and activates mitogen-activated protein kinase pathways in Chinese hamster ovary cells. *Endocrinology* **140:** 1132-1140.

Orskov C, Rabenhoj L, Wettergren A, Kofod H, and Holst JJ (1994) Tissue and plasma concentrations of amidated and glycine-extended glucagon-like peptide I in humans. *Diabetes* **43:** 535-539.

Reimann F, Ward PS, and Gribble FM (2006) Signaling mechanisms underlying the release of glucagon-like peptide 1. *Diabetes* **55** (Suppl. 2): S78-85.

Seidel MG, Klinger M, Freissmuth M, and Holler C (1999). Activation of mitogen-activated protein kinase by the A_2A-adenosine receptor via a rap1-dependent and via a p21ras-dependent pathway. *J Biol Chem* **274:** 25833-25841.

Shigeto M, Katsura M, Matsuda M, Ohkuma S, and Kaku K (2008) Low, but physiological, concentration of GLP-1 stimulates insulin secretion independent of the cAMP-dependent protein kinase pathway. *J Pharmacol Sci* **108:** 274-279.

Syme CA, Zhang L, Bisello A (2006) Caveolin-1 regulates cellular trafficking and function of the glucagon-like peptide 1 receptor. *Mol Endocrinol* **20:** 3400-3411.

Thorens B, Porret A, Buhler L, Shao-Ping D, Morel P, and Widmann C (1993) Cloning and functional expression of the human islet GLP-1 receptor: demonstration that exendin-4 is an agonist and exendin-(9-39) an antagonist of the receptor. *Diabetes* **42:** 1678-1682.

Tovey SC, and Willars GB (2004) Single-cell imaging of intracellular Ca^{2+} and phospholipase C activity reveals that RGS 2, 3 and 4 differentially regulate signaling via the $G\alpha_{q/11}$-linked muscarinic M_3 receptor. *Mol Pharmacol* **66:** 1453-1464.

Vázquez P, Roncero I, Blázquez E, and Alvarez E (2005) The cytoplasmic domain close to the transmembrane region of the glucagon-like peptide-1 receptor contains sequence elements that regulate agonist-dependent internalisation. *J Endocrinol* **186:** 221-231.

Werry TD, Christie MI, Dainty IA, Wilkinson GF, and Willars GB (2003) Cross talk between $P2Y_2$ nucleotide receptors and CXC chemokine receptor 2 resulting in enhanced Ca^{2+} signalling involves enhancement of phospholipase C activity and is enabled by incremental Ca^{2+} release in human embryonic kidney cells. *J Pharmacol Exp Ther* **307:** 661-669.

Wheeler MB, Lu M, Dillon JS, Leng XH, Chen C, and Boyd AE (1993) Functional expression of the rat glucagon-like peptide-1 receptor, evidence for coupling to both adenylyl cyclase and phospholipase-C. *Endocrinology* **133:** 57-62.

Widmann C, Burki E, Dolci W, and Thorens B (1994) Signal transduction by the cloned glucagon-like peptide-1 receptor: comparison with signaling by the endogenous receptors of β cell lines. *Mol Pharmacol* **45:** 1029-1035.

Widmann C, Dolci W, and Thorens B (1995) Agonist-induced internalization and recycling of the glucagon-like peptide-1 receptor in transfected fibroblasts and in insulinomas. *Biochem J* **310:** 203-214.

Willars GB, and Nahorski SR (1995) Quantitative comparisons of muscarinic and bradykinin receptor-mediated Ins(1,4,5)P_3 accumulation and Ca^{2+} signalling in human neuroblastoma cells, *Br J Pharmacol* **114:** 1133-1142.

Footnotes

This study was funded by AstraZeneca, Alderely Park Macclesfield, U.K. with a contribution from the Biotechnology and Biological Sciences Research Council (BBSRC) through a Doctoral Training Grant [BB/D526510/1] (*Y.H.*) awarded to the School of Biological Sciences at the University of Leicester.

JPET Fast Forward. Published on May 27, 2010 as DOI: 10.1124/jpet.110.166009
This article has not been copyedited and formatted. The final version may differ from this version.

Legends for Figures

Fig. 1. GLP-1 couples the GLP-1R to $G\alpha_s$-proteins and induces cAMP generation in HEK-GLP-1R cells. a) Membranes from HEK-GLP-1R cells were incubated in the presence of 1μM ($G\alpha_s$, $G\alpha_{q/11}$) or 10μM ($G\alpha_{i/o}$) GDP and 1nM [^{35}S]-GTPγS and then either treated with vehicle (KHB; Basal) or challenged with 30nM GLP-1 7-36 amide for 5 min. Non-specific binding (NSB) was determined in the presence of 10μM GTPγS. Immunoprecipitation was carried out using antibodies against specific Gα-subunits as indicated and associated [^{35}S] levels determined. For ***, $p<0.001$ (by Bonferroni's test following one-way ANOVA; for clarity, only GLP-1 vs. Basal comparisons are shown). b**)** HEK-GLP-1R cells were treated for the indicated times up to 90 min with either 30nM GLP-1 7-36 amide or vehicle (KHB; Basal) in the absence of IBMX and intracellular levels of cAMP determined and expressed relative to cellular protein content. c) HEK-GLP-1R cells were pre-treated for 10 min with either the GLP-1R antagonist exendin 9-39 (100nM) or vehicle (KHB; Basal) in the presence of IBMX (500μM) before being challenged for 10 min with the indicated concentrations of GLP-1 7-36 amide. Intracellular levels of cAMP were determined and expressed relative to cellular protein content. In the absence and presence of exendin 9-39 respectively, the pEC_{50} values were 10.07±0.14 and 9.60±0.10, the E_{max} values were 1619±90 and 1549±124 pmol/mg protein and the Hill slope values (nH) were 1.19±0.10 and 1.63±0.31. For ***, $p<0.001$ for control curves versus exendin 9-39 pre-treated curves (by two-way ANOVA). d) HEK-GLP-1R cells were either pre-treated with vehicle (Control) or 2μg/ml of cholera toxin for 24 h. In the presence of IBMX (500μM) they were then either treated with vehicle (KHB; Basal) or challenged with GLP-1 7-36 amide (0.1 or 100nM) for 10 min and levels of

intracellular cAMP determined relative to cellular protein content. For **, $p<0.01$ by Student's t-test. Within the figure all data are mean±S.E.M., n≥3.

Fig. 2. GLP-1-mediated Ca^{2+} responses in HEK-GLP-1R cells. HEK-GLP-1R cells were grown in 96-well plates and loaded with the calcium indicator fluo-4. Cells were then challenged with GLP-1 7-36 amide or KHB ('0') and changes in fluorescence recorded using a microplate reader as an index of changes in $[Ca^{2+}]_i$. a) Representative family of traces induced by GLP-1 7-36 amide, which was added at the time indicated by the arrow at 0-10nM. b) Cells were pre-treated for 1 h with either 100nM exendin 9-39 or KHB (Control) and then challenged with either vehicle (KHB; Basal) or the indicated concentrations of GLP-1 7-36 amide. The maximum change in fluorescence units (FU) was determined in each instance to allow generation of concentration-response curves. The pEC_{50} values were 10.18±0.16 for GLP-1 7-36 amide alone and 9.79±0.11 in the presence of exendin 9-39. All data are mean±S.E.M., n=3; **, $p<0.01$ for control curves versus exendin 9-39 pre-treated curves (by two-way ANOVA). c) Cells were either treated as normal (Control), washed and treated in KHB without Ca^{2+} ($-Ca^{2+}_e$), or pre-treated with 2μM thapsigargin for 5 min. Maximal responses following addition of 10nM GLP-1 7-36 amide were then recorded and expressed relative to control samples. Data are mean+S.E.M., n=3-4; ***$p<0.001$ (by Bonferroni's test following one-way ANOVA, with statistical analysis performed on the raw data). d) Cells were pre-treated with either the putative inhibitor of phospholipase C, U73122, or its aminosteroid negative control, U73343, (both 30 min pre-treatment, 10μM) or alternatively treated for 20 h with pertussis toxin (PTX; 100ng/ml). Maximal responses following addition of 100nM GLP-1 7-36 amide were then recorded and expressed relative to control

samples. Stimulations with GLP-1 7-36 amide in the presence of either U73122 or U73343 were performed in the absence of extracellular Ca^{2+}. Data are mean+S.E.M., n=3-6. e) Cells were grown on glass coverslips, loaded with fluo-4 and imaged by confocal microscopy. Cells were then challenged with 1nM GLP-1 7-36 amide. Traces are representative of at least four independent experiments.

Fig. 3. Compound 2 couples the GLP-1R to $G\alpha_s$- but not $G\alpha_{q/11}$- or $G\alpha_{i/o}$-proteins. Membranes from HEK-GLP-1R or HEK-Flp-In cells were incubated in the presence of 1μM ($G\alpha_s$, $G\alpha_{q/11}$) or 10μM ($G\alpha_{i/o}$) GDP and 1nM [^{35}S]-GTPγS and then challenged with agonist or vehicle (5% v/v DMSO; Basal) where appropriate for 5 min. Non-specific binding (NSB) was determined using 10μM GTPγS (and subtracted from values in (a)). Immunoprecipitation was carried out using antibodies against specific Gα-subunits as indicated and associated [^{35}S] levels determined. a-c) Membranes from HEK-GLP-1R cells were stimulated with the indicated concentrations of compound 2 and a $G\alpha_s$ (a), $G\alpha_{q/11}$ (b) or $G\alpha_{i/o}$ (c)-specific antibody used for immunoprecipitation. The pEC_{50} for the rising phase in (a) was 5.36±0.16 (4.4μM). Using the $G\alpha_s$ antibody the response to 30nM GLP-1 was 1506±128 c.p.m. (with NSB subtracted) whereas the maximal response to compound 2 was 245±32 c.p.m. d) Membranes from HEK-Flp-In cells were stimulated with either vehicle (Basal), compound 2 (10μM) or GLP-1 7-36 amide (30nM) and a $G\alpha_s$-specific antibody used for immunoprecipitation. Data are mean±/+S.E.M., n=3-4.

Fig. 4. Compound 2 induces cAMP generation in HEK-GLP-1R cells. HEK-GLP-1R or HEK-Flp-In cells were challenged with either vehicle (Basal), forskolin, compound 2 or GLP-1 7-36 amide in the presence of IBMX (500μM) unless otherwise stated.

Levels of intracellular cAMP were determined relative to the cellular protein content. The final concentration of DMSO (vehicle) was 5% v/v in all cases. a) HEK-GLP-1R cells were treated with vehicle (Basal) or the indicated concentrations of compound 2 for 10 min; the pEC_{50} was 6.23±0.07. The response to 30nM GLP-1 in parallel experiments was 2017±371 pmol cAMP/mg protein. Data are mean±S.E.M., n=3. b) HEK-Flp-In cells were treated for 10 min with vehicle (Basal), forskolin (FSK; 10μM), compound 2 (1 or 10μM) or GLP-1 7-36 amide (30nM). Data are mean+S.E.M., n=3. c) HEK-GLP-1R cells were treated for up to 90 min with 1μM compound 2 or vehicle (Basal) but in the absence of IBMX. Data are mean+S.D. from duplicates within one experiment, representative of two others. d) HEK-GLP-1R cells were treated with vehicle (Basal) or the indicated concentrations of compound 2 for 90 min. Data are mean±S.E.M., n=4.

Fig. 5. Cytotoxic effects of compound 2. a) HEK-GLP-1R cells were treated for 90 min with vehicle (5% v/v DMSO; Basal), GLP-1 7-36 amide, compound 2 (Cpd2) or forskolin (FSK) and both intracellular and extracellular cAMP measured separately as described in Methods. Data are mean+/-S.E.M., n=3. b) HEK-GLP-1R or control (not transfected with the GLP-1R) HEK-Flp-In cells were treated with vehicle (5% v/v DMSO) or compound 2 at the indicated concentrations in the presence of IBMX (500μM) for 90 min, washed and stained with 0.02% trypan blue and viewed with a x40 objective lens. Data are representative images of 3 separate experiments where each treatment was carried out in duplicate. c) HEK-GLP-1R cells were treated with forskolin (100μM) and the indicated concentrations of compound 2 for 90 min in the presence of IBMX (500μM) and 5% v/v DMSO (vehicle) and levels of intracellular cAMP determined relative to cellular protein content. d) Cells were cultured in the

absence (Control) or presence of pertussis toxin (100ng/ml) for ~20 h and then stimulated with forskolin (100μM) in the presence of either vehicle (5% v/v DMSO) or compound 2 (100μM) as in C. All data are mean±/+S.E.M., n=3-4.

Fig. 6. Cholera toxin-sensitivity of GLP-1R-mediated cAMP generation by compound 2. HEK-GLP-1R cells were either pre-treated with vehicle (Control) or 2μg/ml of cholera toxin for ~20 h. Cells were then either challenged with vehicle (5% v/v DMSO; Basal) or compound 2 as indicated in the presence of IBMX (500μM) for 10 min and levels of intracellular cAMP determined relative to cellular protein content. Data are mean+/±S.E.M., n=5 (a) or 3 (b); **, $p<0.01$ by Student's paired t-test (a); *, $p<0.05$, by two-way ANOVA (b); pEC_{50} values 6.10±0.07 (control) and 6.73±0.03 (cholera toxin), $p<0.05$ by Student's paired t-test.

Fig. 7. Functional interaction of compound 2 with exendin 9-39 and GLP-1 7-36 amide. HEK-GLP-1R cells were treated with vehicle (5% v/v DMSO; Basal), compound 2 or GLP-1 7-36 amide in the presence of IBMX (500μM) and levels of intracellular cAMP determined relative to cellular protein content. a) Cells were pre-treated for 10 min with either exendin 9-39 (100nM) or KHB (Control) and then stimulated with the indicated concentrations of compound 2 for 10 min. ***, $p<0.001$ versus control by two-way ANOVA. b) Cells were pre-treated for 10 min with exendin 9-39 (0.1-3μM) or KHB (Control) and then challenged with vehicle (5% v/v DMSO) submaximal concentrations of either GLP-1 7-36 amide (100pM) or compound 2 (1μM) for 10 min. *, $p<0.05$; **, $p<0.01$, ***; $p<0.001$ compared to control by Dunnett's test following one-way ANOVA. c) Cells were treated for 10 min with either vehicle (5% v/v DMSO) or compound 2 at the indicated

concentrations and either buffer (KHB; 0) or GLP-1 7-36 amide at the concentrations indicated on the abscissa. The pEC$_{50}$ values for GLP-1 7-36 amide-mediated cAMP generation in the presence of the different concentrations of compound 2 are given in the table; $p<0.05$ for these values by F-test. All data are mean±/+S.E.M., n=3-4.

Fig. 8. Compound 2-mediated Ca^{2+} signaling. Cells were grown in 96-well plates and loaded with the Ca^{2+} indicator fluo-4. Cells were then challenged with either vehicle (5% v/v DMSO), compound 2 or GLP-1 7-36 amide as indicated and changes in fluorescence recorded using a microplate reader as an index of changes in $[Ca^{2+}]_i$. a) Representative traces showing Ca^{2+} responses in HEK-GLP-1R cells. b) Maximal Ca^{2+} responses to the indicated concentrations of compound 2, vehicle (5% v/v DMSO) or GLP-1 7-36 amide in HEK-GLP-1R cells. c) Representative traces following addition of GLP-1 7-36 amide, compound 2 or vehicle to HEK-Flp-In cells. d) HEK-GLP-1R cells were either treated as normal (Control), washed and treated in KHB without Ca^{2+} (-Ca^{2+}_e), or pre-treated with 2μM thapsigargin for 5 min. Maximal responses following addition of 100μM compound 2 were then determined. Traces are either representative of n=3-4 or mean+S.E.M., n=3-4; ***$p<0.001$ (by Bonferroni's test following one-way ANOVA). e) HEK-GLP-1R cells were pre-treated with either U73122 or U73343 (30 min pre-treatment, 10μM) or alternatively treated for 20 h with pertussis toxin (PTX; 100ng/ml). Maximal responses following addition of 30μM compound 2 were then recorded and expressed relative to control samples. Stimulations with compound 2 in the presence of either U73122 or U73343 were performed in the absence of extracellular Ca^{2+}. Data are mean+S.E.M., n=3-5.

Fig. 9. GLP-1 7-36 amide- and compound 2-mediated cAMP generation in HEK-GLP-1R cells and cells with stable expression of an EGFP-tagged GLP-1R. A cell line was generated with stable expression of a C-terminally tagged GLP-1R (HEK-GLP-1R-EGFP) and either these or HEK-GLP-1R cells challenged with either GLP-1 7-36 amide (open squares (□) and closed squares (■) respectively) or compound 2 (open circles (○) and closed circles (●) respectively) at the indicated concentrations for 10 min in the presence of IBMX (500μM). Levels of intracellular cAMP were determined relative to the cellular protein content and are expressed in relation to the maximal response generated by GLP-1 7-36 amide in HEK-GLP-1R cells. Whenever compound 2 was used, the final concentration of DMSO (vehicle) was 5% v/v in all cases. The pEC_{50} values were: HEK-GLP-1R, 10.40±0.27 and 6.00±0.13 for GLP-1 7-36 amide and compound 2 respectively; HEK-GLP-1R-EGFP, 10.41±0.18 and 6.02±0.03 GLP-1 7-36 amide and compound 2 respectively.

Fig. 10. Agonist-mediated internalisation of the GLP-1R. a) HEK-GLP-1R-EGFP were imaged by confocal microscopy over a 60 min period during which time they were challenged with: GLP-1 7-36 amide (GLP-1, 100nM) in the absence or presence of exendin 9-39 (Ex 9-39, 100nM); compound 2 (Cpd2, 10μM) in the absence or presence of exendin 9-39 (100nM); GLP-1 7-36 amide (100nM) and compound 2 (10μM) (panel B only); exendin 9-39 (100nM) (panel B only) and; DMSO (0.1% v/v; Basal) as indicated. Images were taken periodically over the 60 min period and shown here are images representative of 3 experiments showing the distribution of EGFP fluorescence at 0, 5, 10, 30 and 60 min. The scale bar in the bottom left of the first image in each row represents 5μm. b) Using the procedure described in the

Methods, an index of internalisation was derived from 6 randomly chosen cells for each condition in each of three independent experiments. Data are mean+S.D., n=18.

Fig. 11. Enhancement of compound 2-mediated cAMP generation by exendin 9-39. a) Intact HEK-GLP-1R-EGFP cells were pre-treated for 10 min with either exendin 9-39 (100nM) or vehicle (KHB) in the presence of IBMX (500μM) before challenge for 5 min with the indicated concentrations of GLP-1 7-36 amide (squares (■, □)) or compound 2 (circles (●,○)) in the continued absence (filled symbols (■,●) or presence of exendin 9-39 (open symbols (□,○)). When compound 2 was used, the final concentration of DMSO (vehicle) was 5% v/v. Levels of intracellular cAMP were determined relative to the cellular protein content. The pEC_{50} values were: GLP-1 7-36 amide, 10.20±0.09 and 9.65±0.10 in the absence and presence of exendin 9-39 respectively; compound 2, 5.36±0.04 and 5.61±0.07 in the absence and presence of exendin 9-39 respectively. b**)** Membranes were prepared from HEK-GLP-1R cells and unchallenged (Basal) or challenged with either forskolin (FSK, 10μM) or GTP (10μM). Alternatively, membranes were challenged with either GLP-1 7-36 amide (10nM) or compound 2 (Cpd 2, 100μM). For each of the conditions, membranes were challenged in the presence of IBMX in the absence (0) or presence of exendin 9-39 (0.1 or 1μM) as indicated. Reactions were terminated after 5 min at 30°C and cAMP levels determined and expressed relative to membrane protein. The concentration of GLP-1 7-36 amide used (10nM) was sub-maximal as 100nM generated 8742±133 pmol/mg protein cAMP. All data are mean±/+S.E.M., n=≥4, for ***, $p<0.001$ by Dunnett's test following one-way ANOVA.

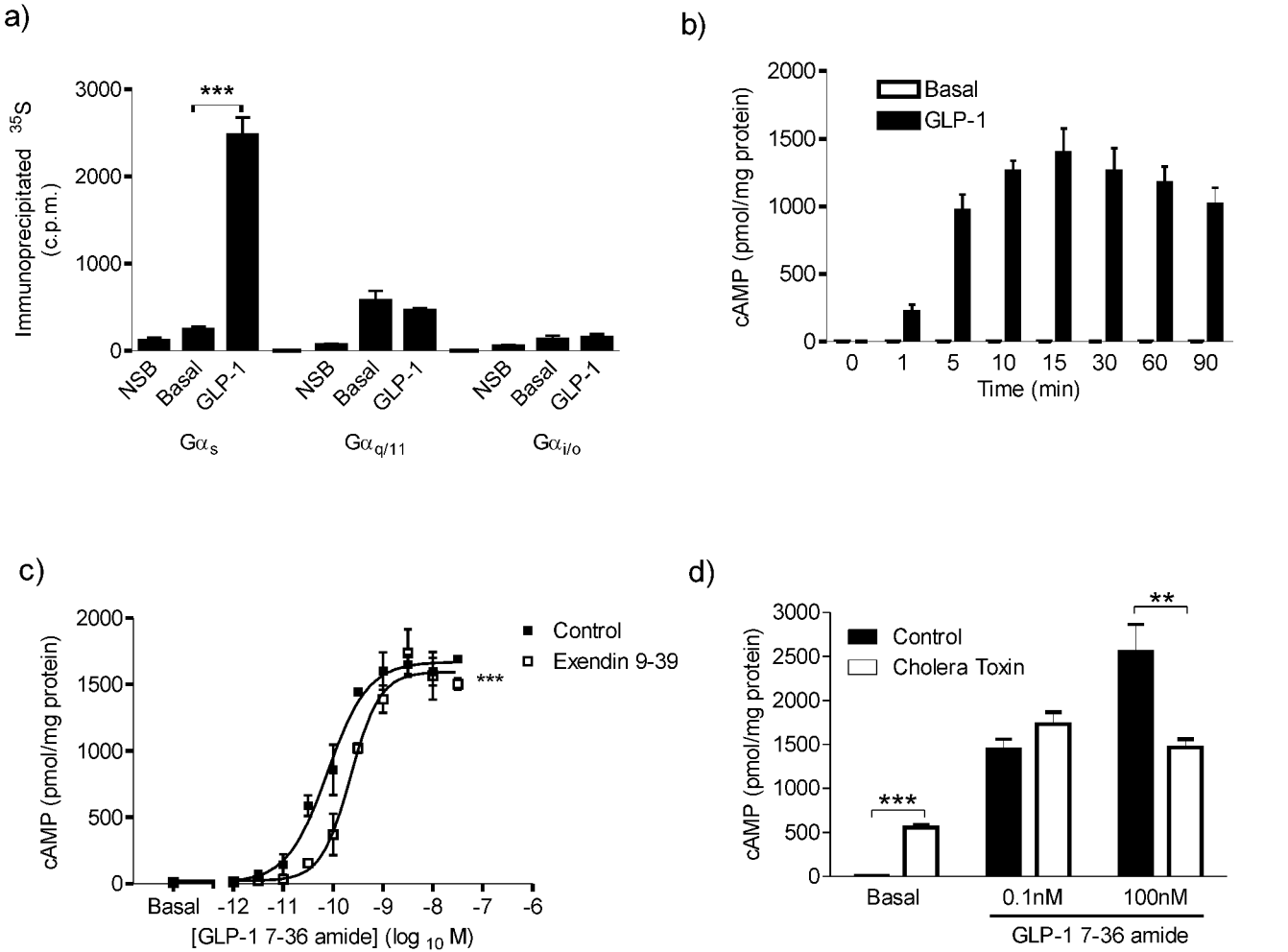
a)
Immunoprecipitated ^{35}S (c.p.m.)
3000
2000
1000
0
***
NSB
Basal
GLP-1
$G\alpha_s$
$G\alpha_{q/11}$
$G\alpha_{i/o}$
b)
cAMP (pmol/mg protein)
2000
1500
1000
500
0
Basal
GLP-1
0
1
5
10
15
30
60
90
Time (min)
c)
cAMP (pmol/mg protein)
Control
Exendin 9-39
***
Basal
-12
-11
-10
-9
-8
-7
-6
[GLP-1 7-36 amide] (log $_{10}$ M)
d)
cAMP (pmol/mg protein)
Control
Cholera Toxin
***
**
Basal
0.1nM
100nM
GLP-1 7-36 amide

Fig. 1.

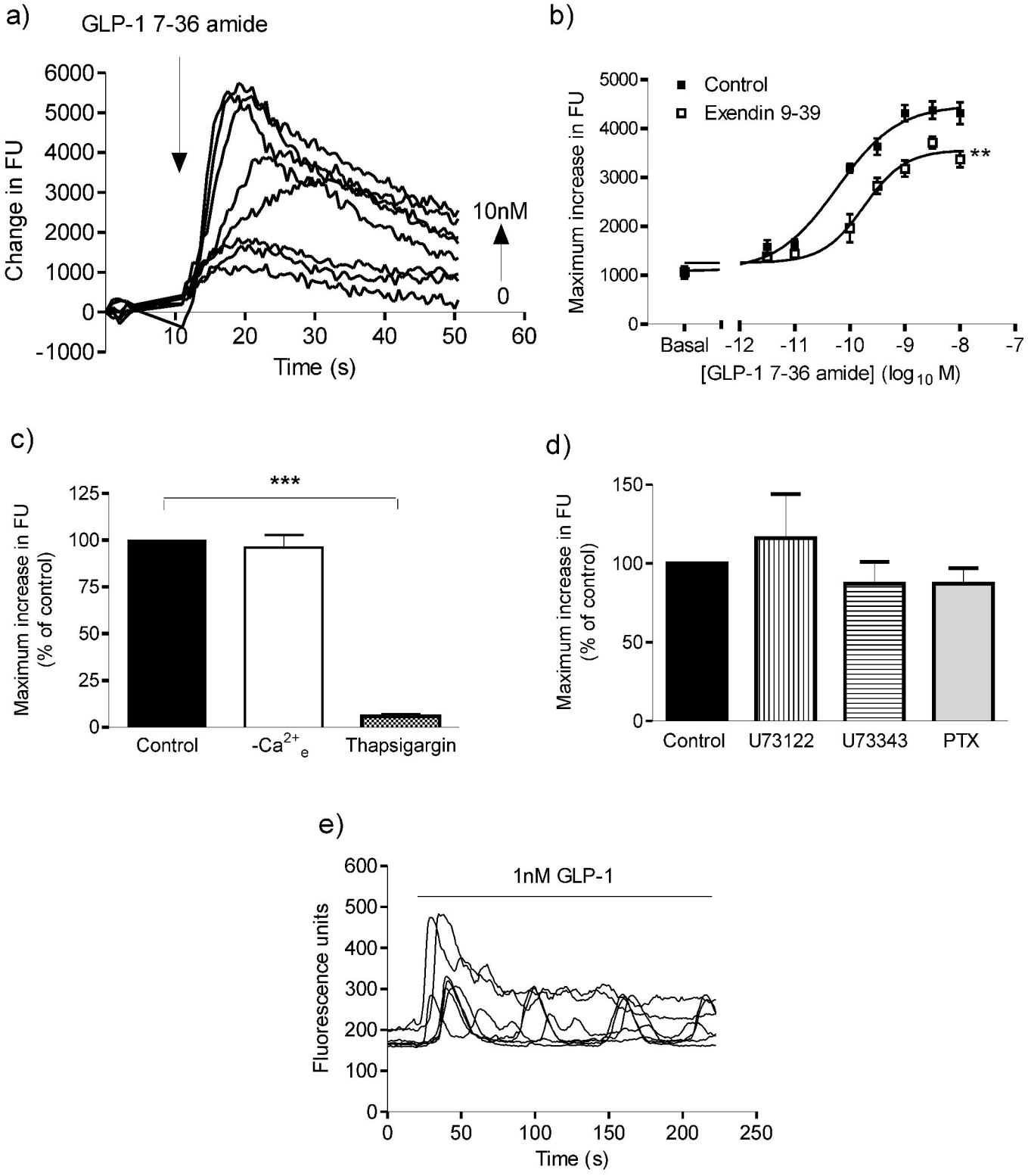
a)
GLP-1 7-36 amide
Change in FU
Time (s)
10nM
0
b)
Control
Exendin 9-39
Maximum increase in FU
**
Basal
[GLP-1 7-36 amide] (log10 M)
c)
***
Maximum increase in FU (% of control)
Control
-Ca2+e
Thapsigargin
d)
Maximum increase in FU (% of control)
Control
U73122
U73343
PTX
e)
1nM GLP-1
Fluorescence units
Time (s)

Fig. 2.

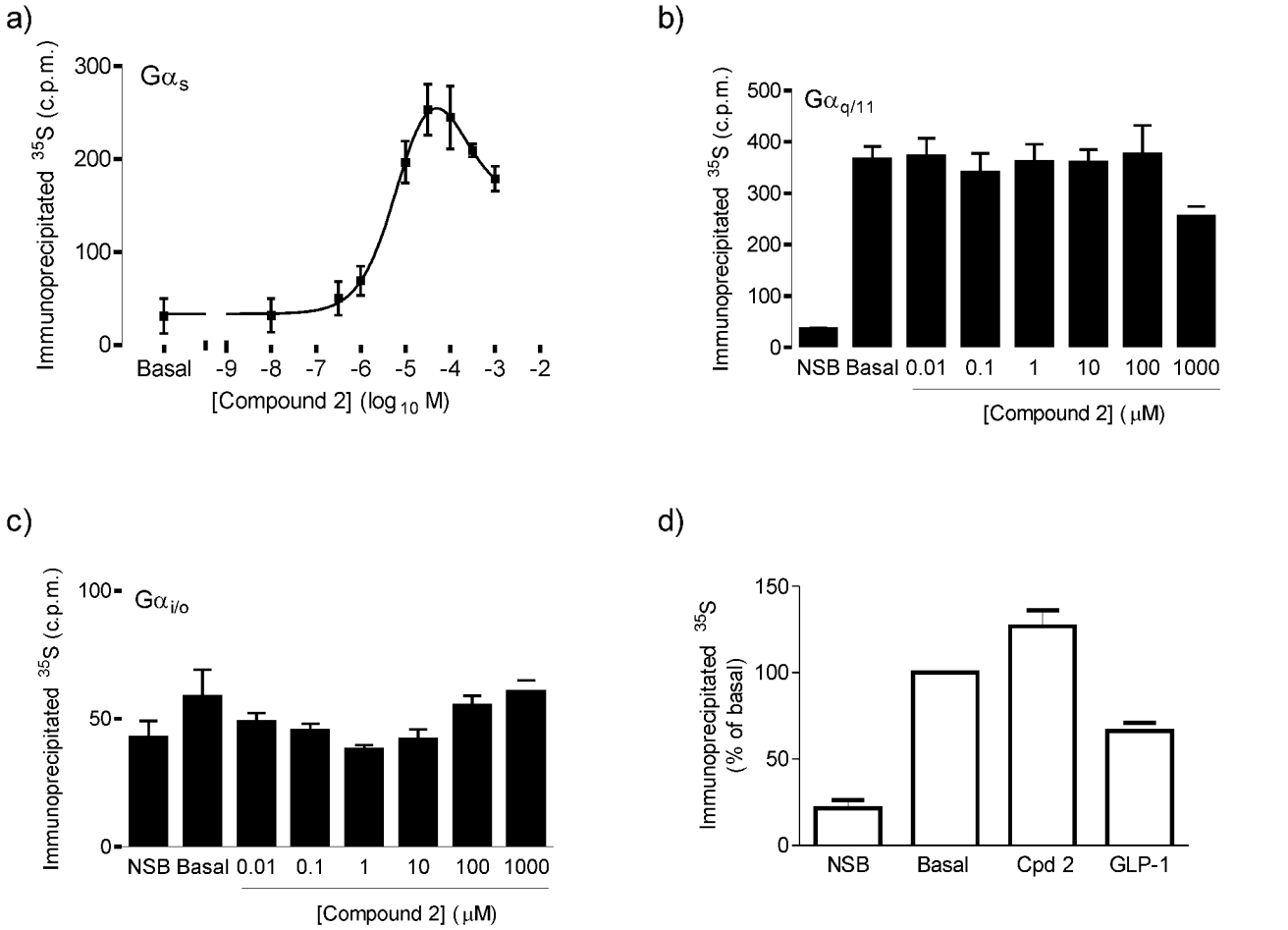
a)
Gαs
Immunoprecipitated 35S (c.p.m.)
300
200
100
0
Basal -9 -8 -7 -6 -5 -4 -3 -2
[Compound 2] (log10 M)
b)
Gαq/11
Immunoprecipitated 35S (c.p.m.)
500
400
300
200
100
0
NSB Basal 0.01 0.1 1 10 100 1000
[Compound 2] (μM)
c)
Gαi/o
Immunoprecipitated 35S (c.p.m.)
100
50
0
NSB Basal 0.01 0.1 1 10 100 1000
[Compound 2] (μM)
d)
Immunoprecipitated 35S (% of basal)
150
100
50
0
NSB
Basal
Cpd 2
GLP-1

Fig. 3.

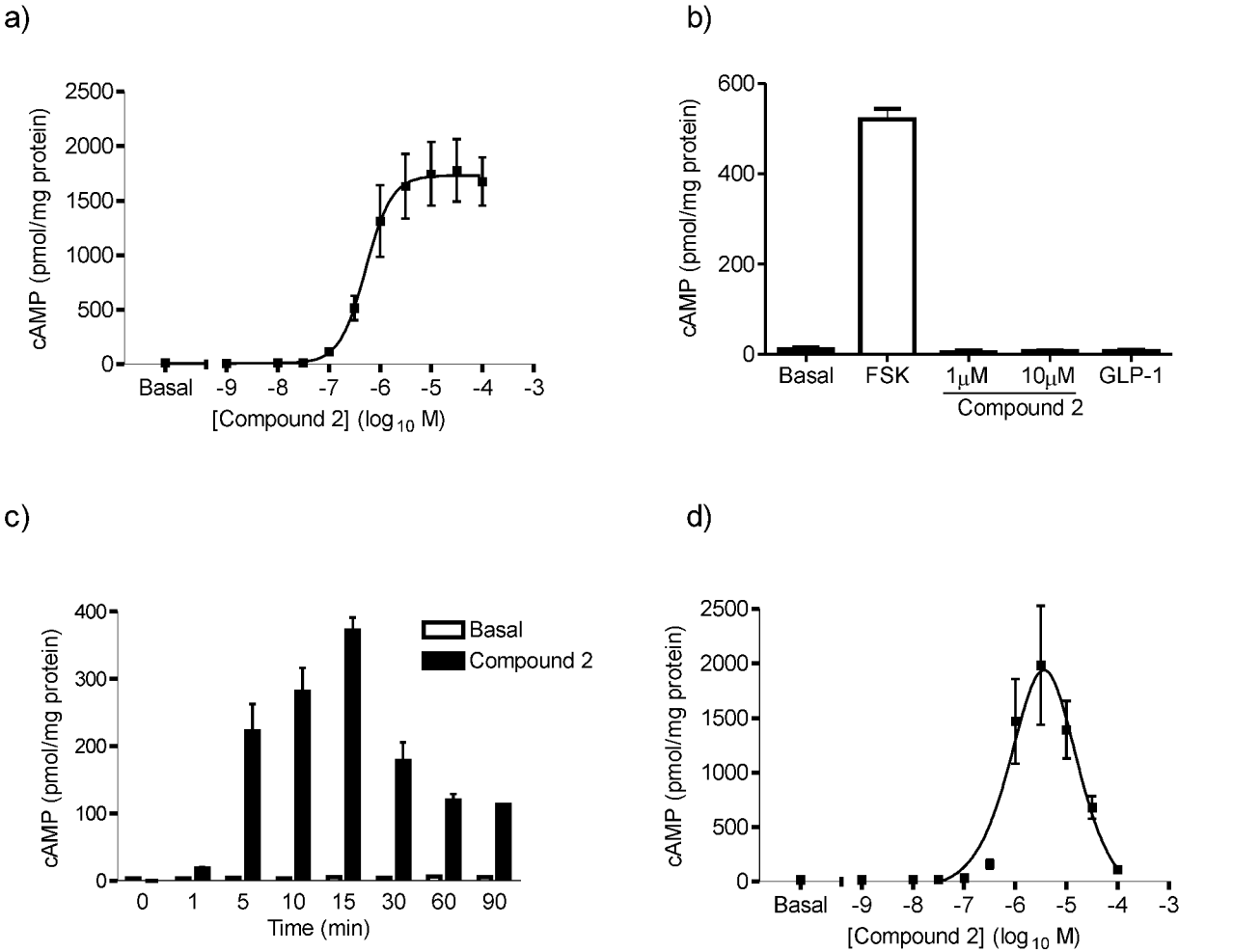
a)
cAMP (pmol/mg protein)
2500
2000
1500
1000
500
0
Basal
-9
-8
-7
-6
-5
-4
-3
[Compound 2] (log 10 M)
b)
cAMP (pmol/mg protein)
600
400
200
0
Basal
FSK
1μM
10μM
GLP-1
Compound 2
c)
cAMP (pmol/mg protein)
400
300
200
100
0
Basal
Compound 2
0
1
5
10
15
30
60
90
Time (min)
d)
cAMP (pmol/mg protein)
2500
2000
1500
1000
500
0
Basal
-9
-8
-7
-6
-5
-4
-3
[Compound 2] (log 10 M)

Fig. 4.

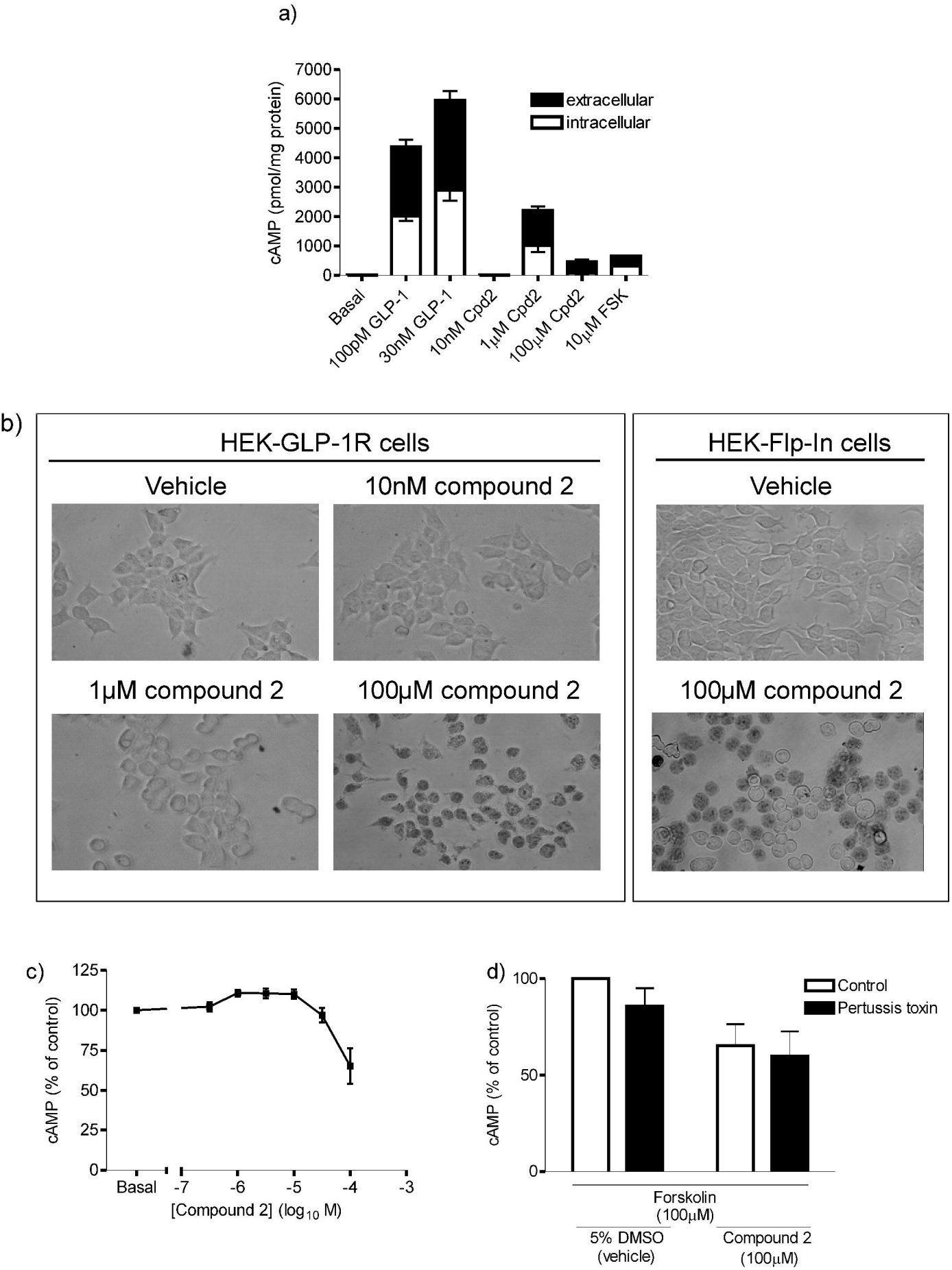
a)
cAMP (pmol/mg protein)
7000
6000
5000
4000
3000
2000
1000
0
extracellular
intracellular
Basal
100pM GLP-1
30nM GLP-1
10nM Cpd2
1μM Cpd2
100μM Cpd2
10μM FSK
b)
HEK-GLP-1R cells
Vehicle
10nM compound 2
1μM compound 2
100μM compound 2
HEK-Flp-In cells
Vehicle
100μM compound 2
c)
cAMP (% of control)
125
100
75
50
25
0
Basal
-7
-6
-5
-4
-3
[Compound 2] (log10 M)
d)
cAMP (% of control)
100
50
0
Control
Pertussis toxin
Forskolin
(100μM)
5% DMSO
(vehicle)
Compound 2
(100μM)

Fig. 5.

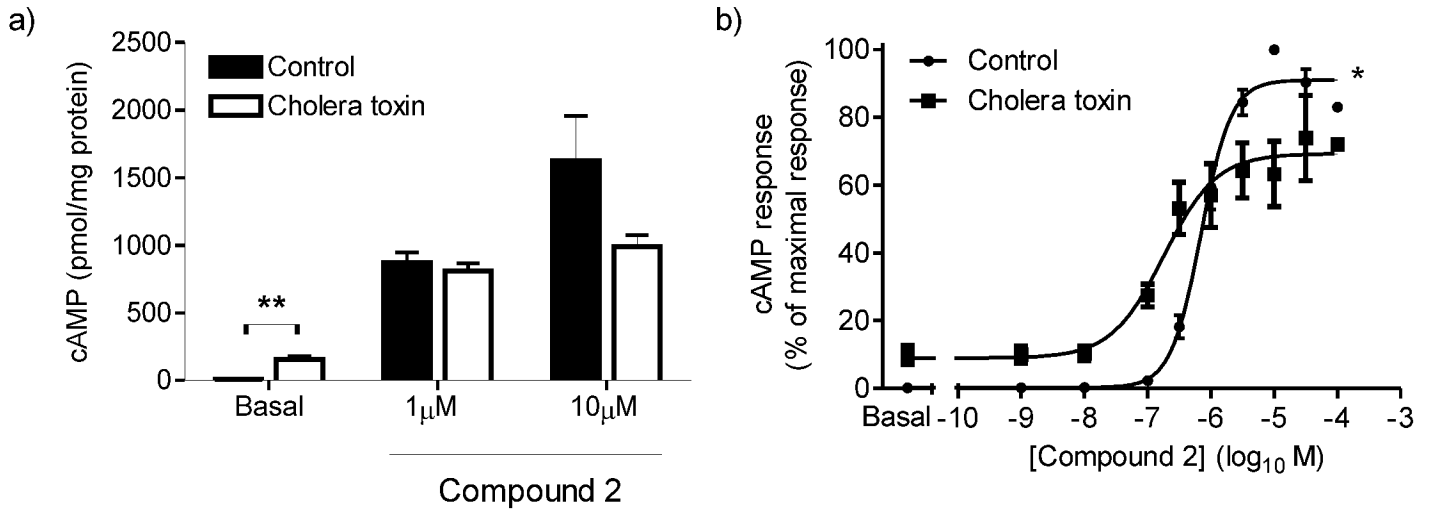
a)
2500
2000
1500
1000
500
0
cAMP (pmol/mg protein)
Control
Cholera toxin
**
Basal
1μM
10μM
Compound 2
b)
100
80
60
40
20
0
cAMP response
(% of maximal response)
Control
Cholera toxin
*
Basal
-10
-9
-8
-7
-6
-5
-4
-3
[Compound 2] (log10 M)

Fig. 6.

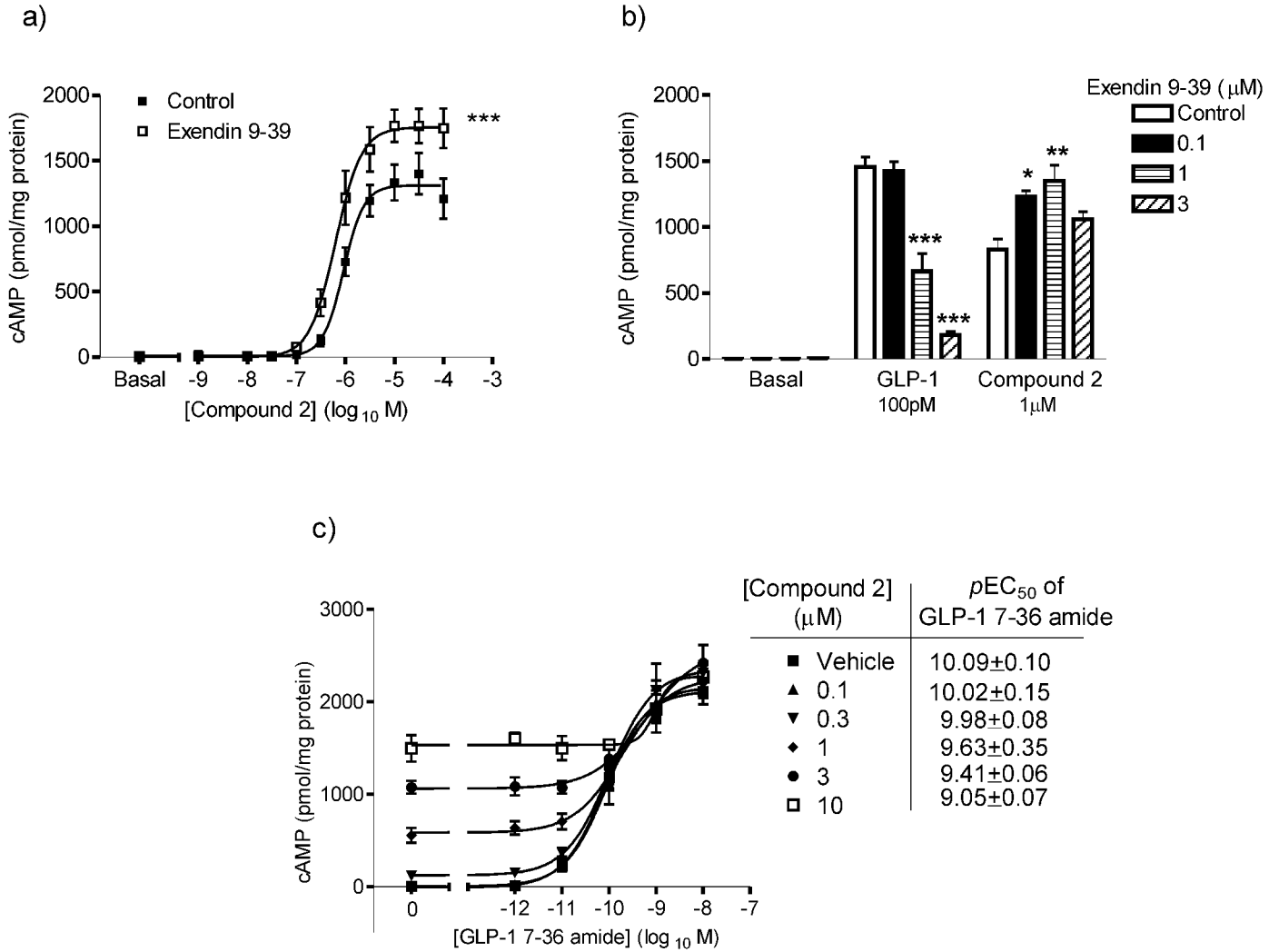
a)
Control
Exendin 9-39
***
cAMP (pmol/mg protein)
2000
1500
1000
500
0
Basal
-9
-8
-7
-6
-5
-4
-3
[Compound 2] (log 10 M)
b)
Exendin 9-39 (μM)
Control
0.1
1
3
cAMP (pmol/mg protein)
***
***
*
**
Basal
GLP-1
100pM
Compound 2
1μM
c)
cAMP (pmol/mg protein)
3000
2000
1000
0
0
-12
-11
-10
-9
-8
-7
[GLP-1 7-36 amide] (log 10 M)
[Compound 2] (μM)
pEC50 of GLP-1 7-36 amide
Vehicle
10.09±0.10
0.1
10.02±0.15
0.3
9.98±0.08
1
9.63±0.35
3
9.41±0.06
10
9.05±0.07

Fig. 7.

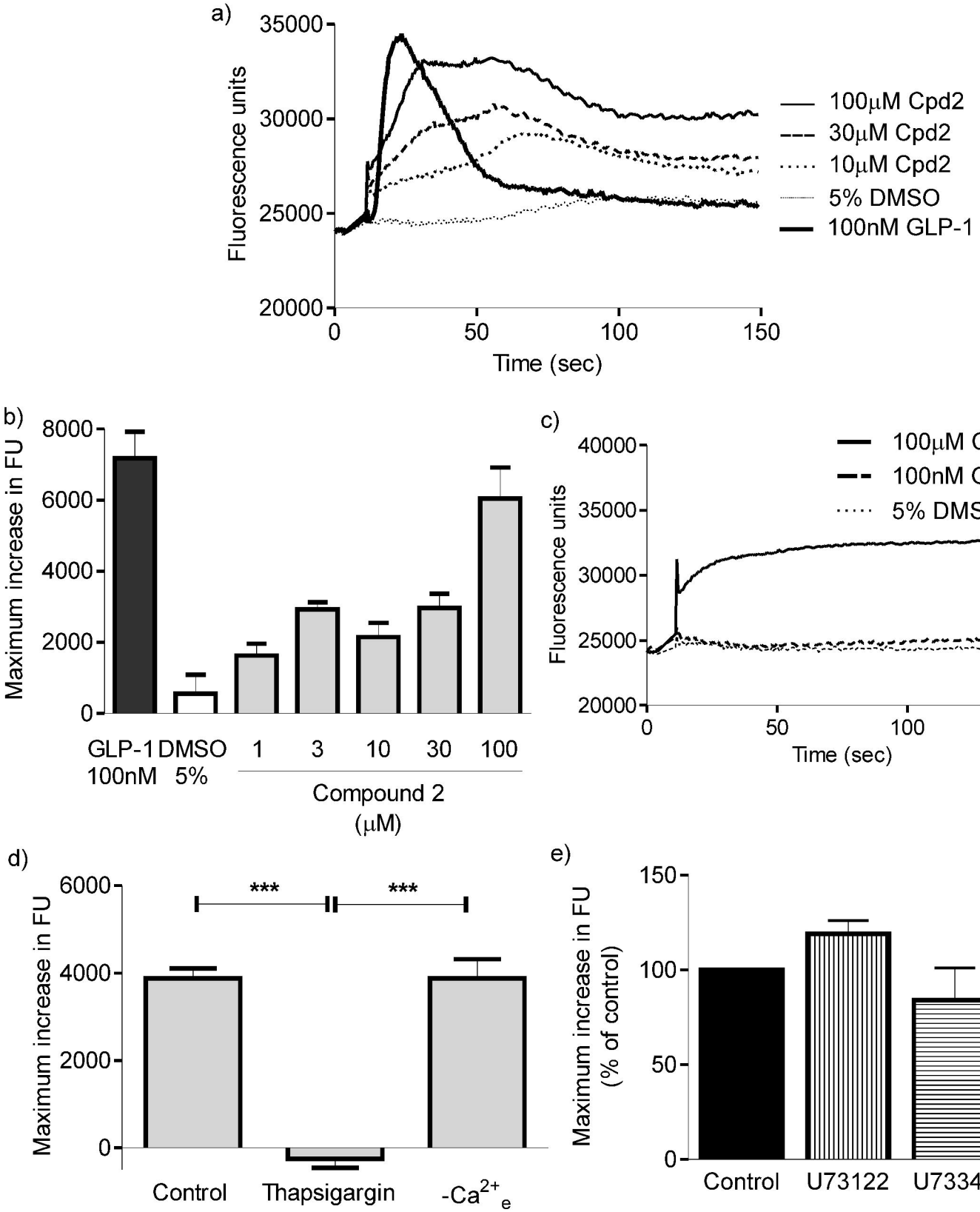

Fig. 8.

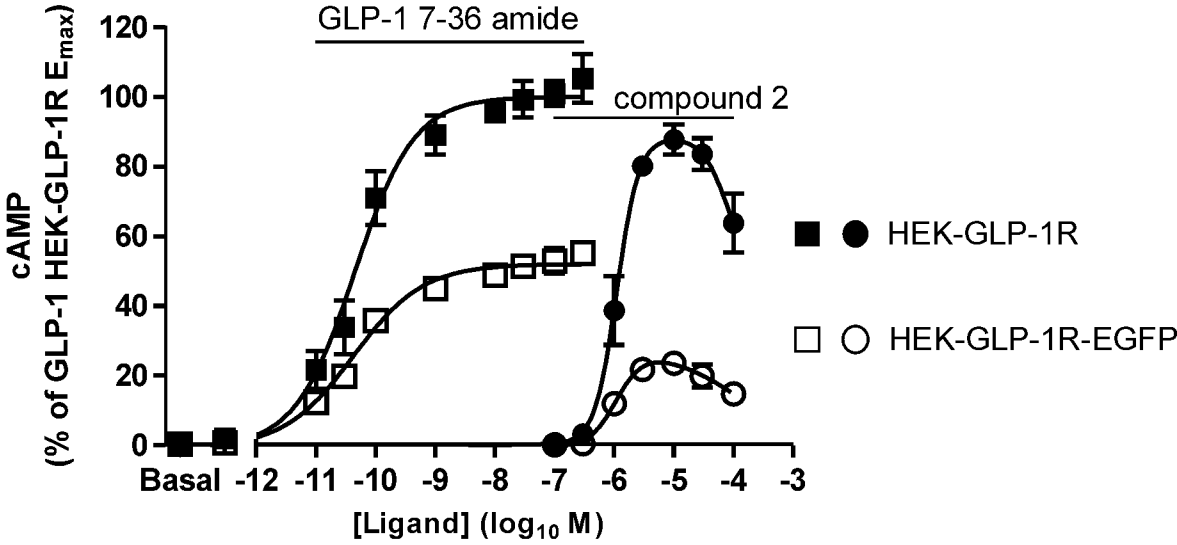
GLP-1 7-36 amide
compound 2
cAMP
(% of GLP-1 HEK-GLP-1R E_{max})
120
100
80
60
40
20
0
Basal -12 -11 -10 -9 -8 -7 -6 -5 -4 -3
[Ligand] (log_{10} M)
HEK-GLP-1R
HEK-GLP-1R-EGFP

Fig. 9.

JPET Fast Forward. Published on May 27, 2010 as DOI: 10.1124/jpet.110.166009
This article has not been copyedited and formatted. The final version may differ from this version.

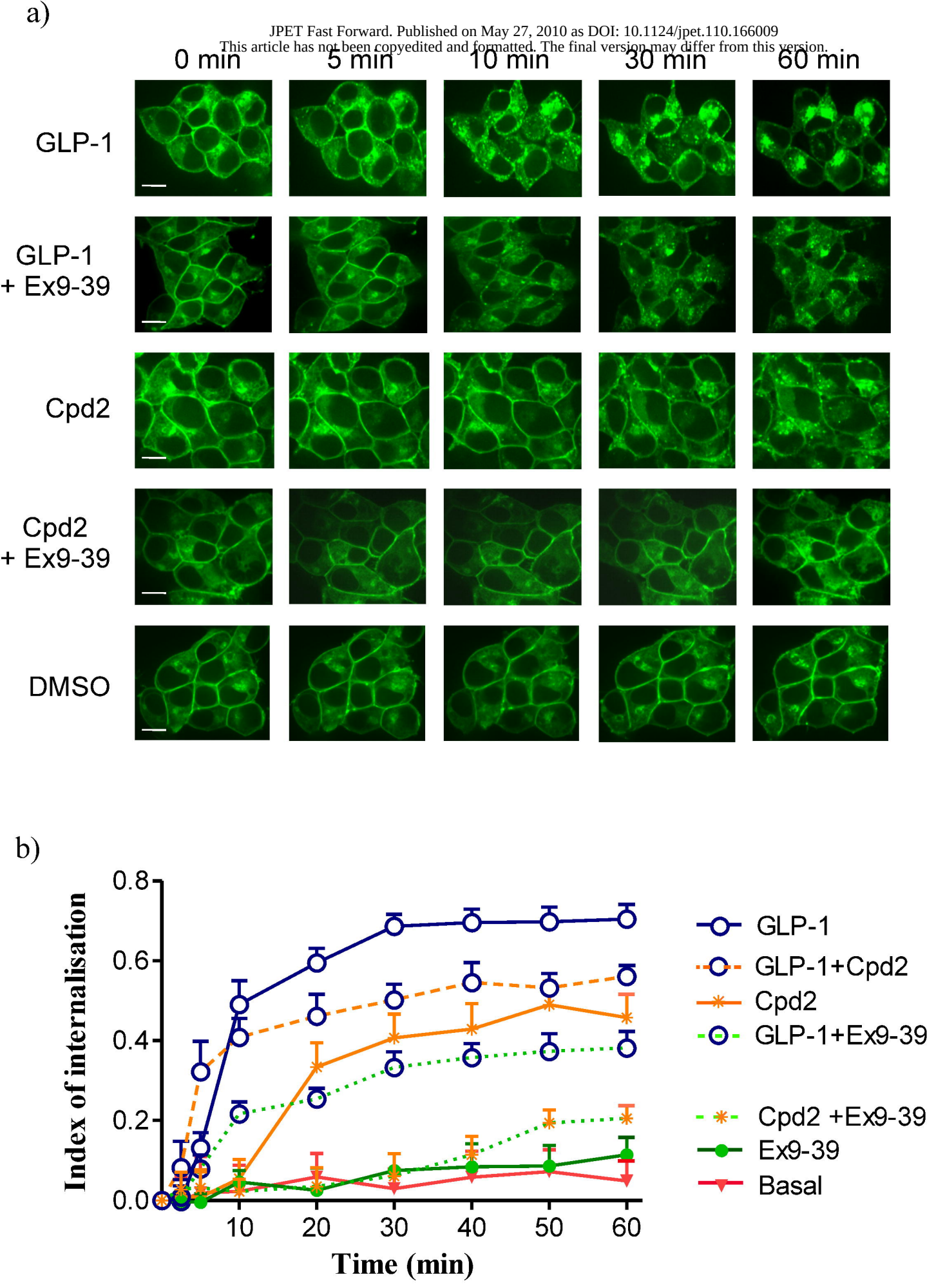

Fig. 10.

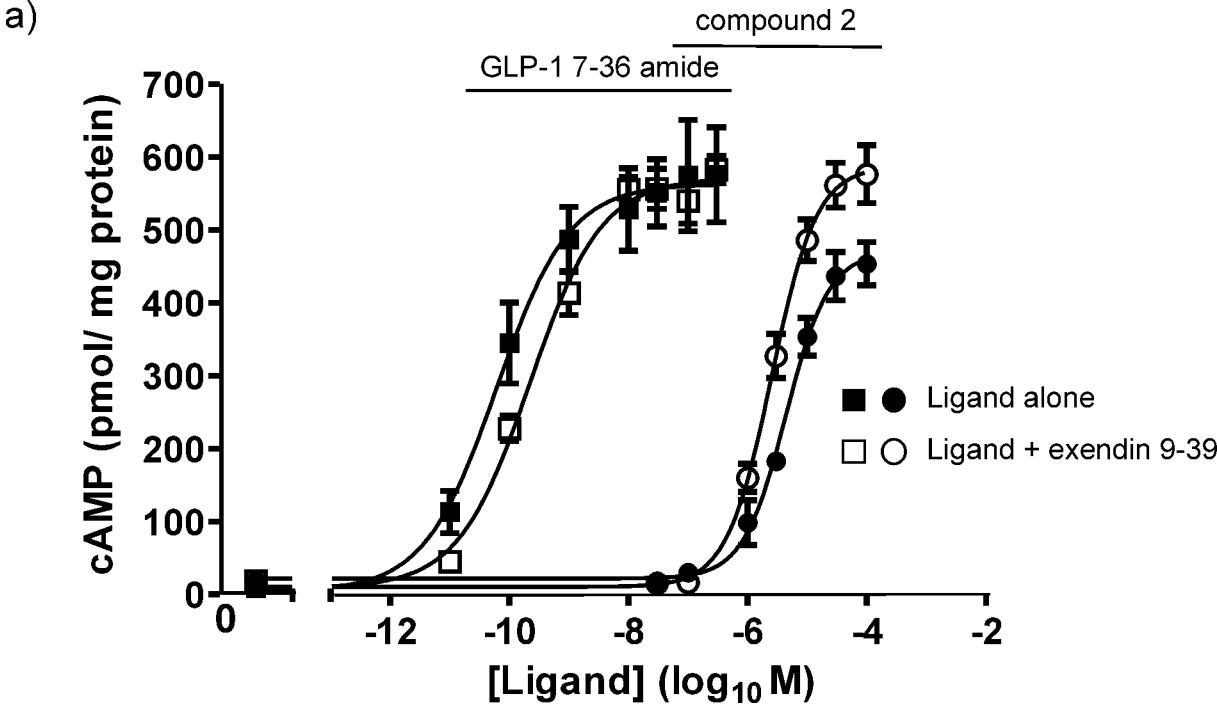
a)
compound 2
GLP-1 7-36 amide
cAMP (pmol/ mg protein)
700
600
500
400
300
200
100
0
0
-12
-10
-8
-6
-4
-2
[Ligand] (log10 M)
Ligand alone
Ligand + exendin 9-39

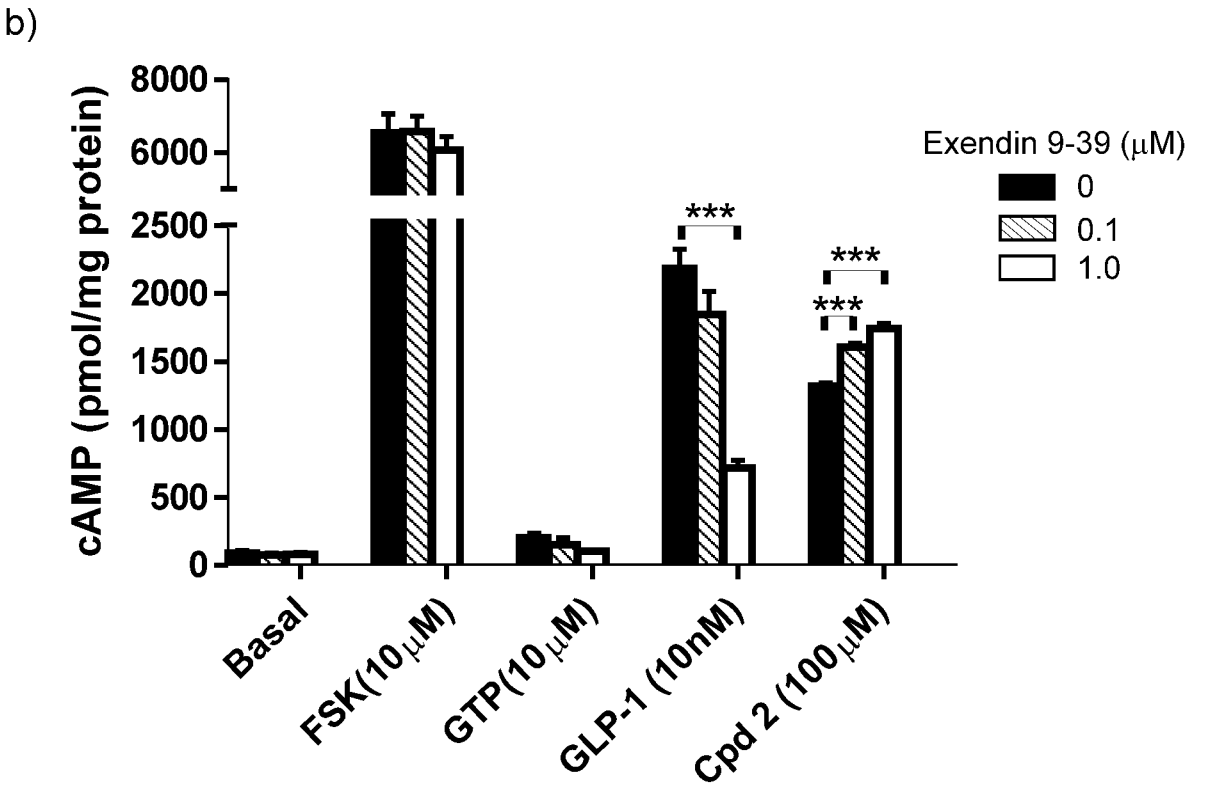
b)
cAMP (pmol/mg protein)
8000
6000
2500
2000
1500
1000
500
0
***
***
***
Exendin 9-39 (μM)
0
0.1
1.0
Basal
FSK(10μM)
GTP(10μM)
GLP-1 (10nM)
Cpd 2 (100μM)

Fig. 11.